

FYS4310

Metallization

FOR THE REST OF US
FOR THE REST OF US

Metallization-outline

What is it used for

Ch 15

Ωic contacts, Schottky barriers, interconnects

Theory M-1/2cond (Ωics, Schottky)

Ch 15

Thin Film metal deposition

Ch 12

Silicides

polySi el prop

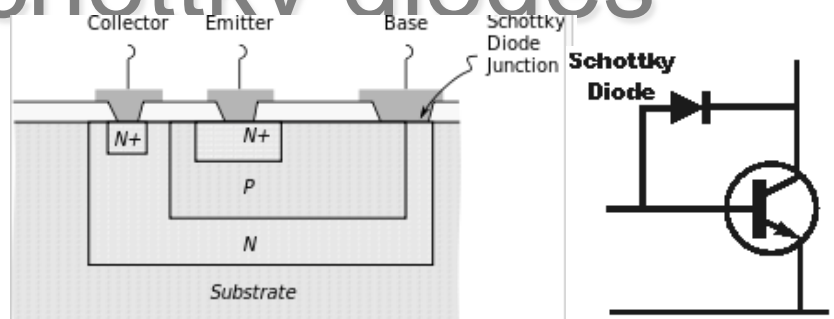
Diffusion, diffusion barriers, electro migration

Ch 15

Ch 12

Uses of Schottky diodes

Clamping diodes in bipolar transistors



Mixer diodes in ultra high frequency devices (InP, GaAs)

Particle detectors (Au/Si)

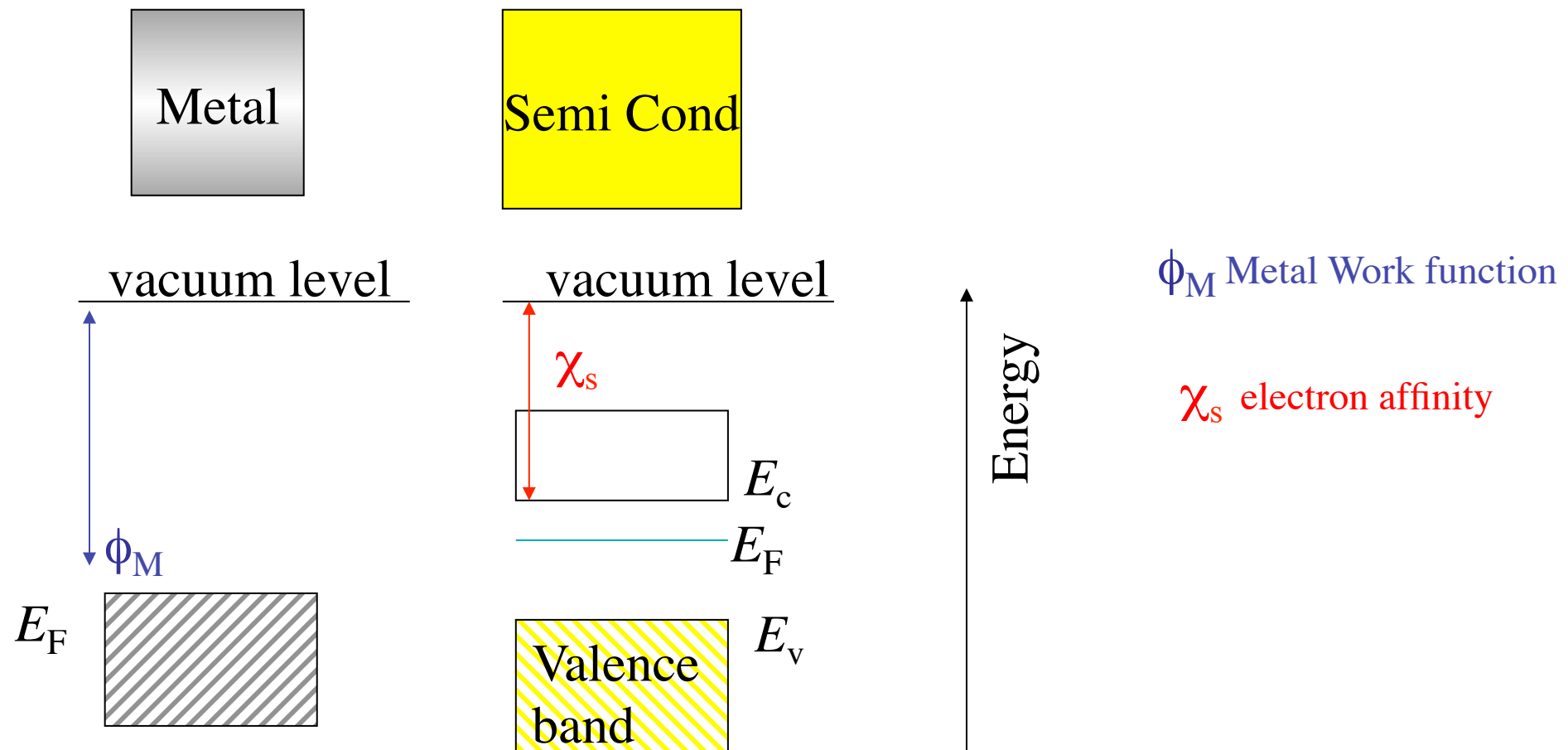
IR detectors (PtSi, Pt_xIr_{1-x}Si arrays)

MESFETs (GaAs)

Diagnostics: CV for carrier conc., DLTS, lifetime etc.

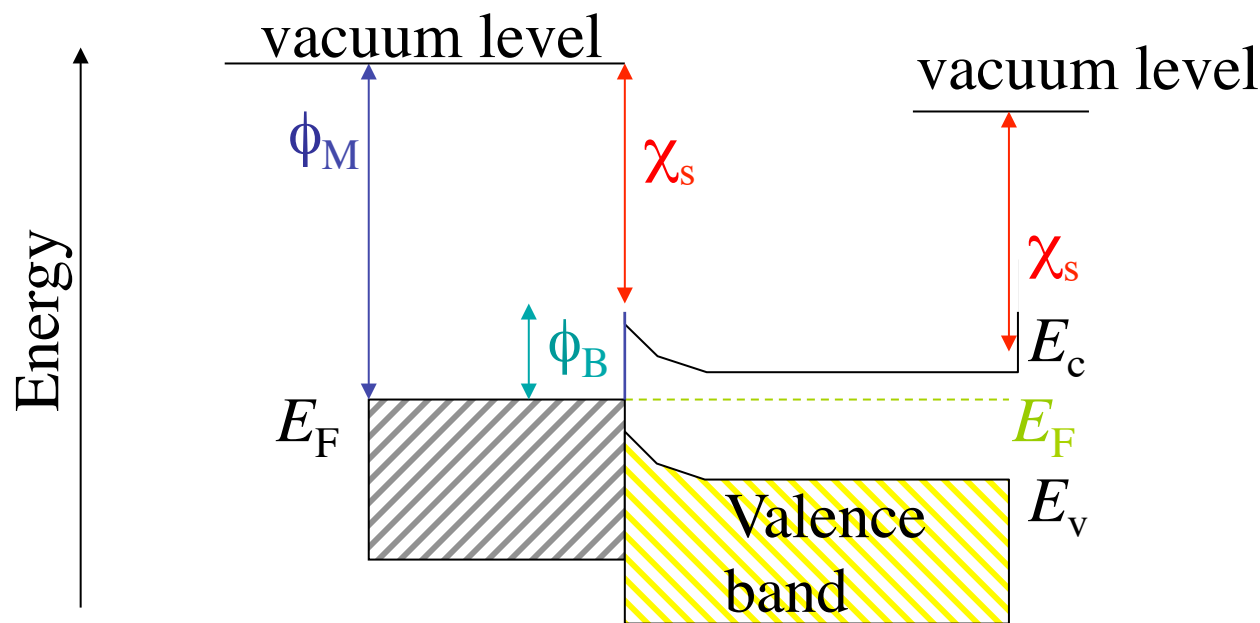
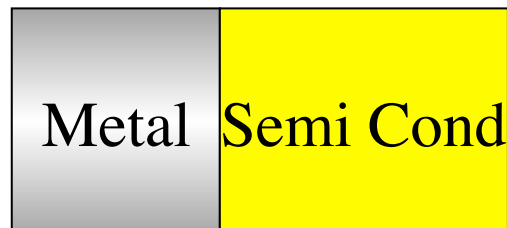
Metal-Semiconductor junctions

Energy band diagrams



Let's connect semiconductor and Metal

Energy band diagrams



ϕ_B Barrier height

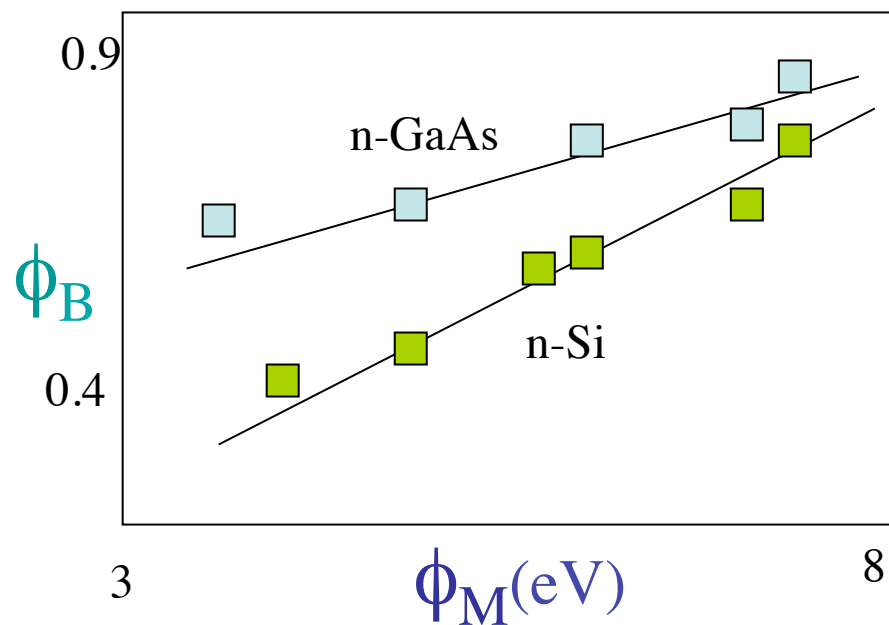
$$\phi_B \neq \phi_M - \chi_s$$

Why(not)?

$$\phi_B \neq \phi_M - \chi_s$$

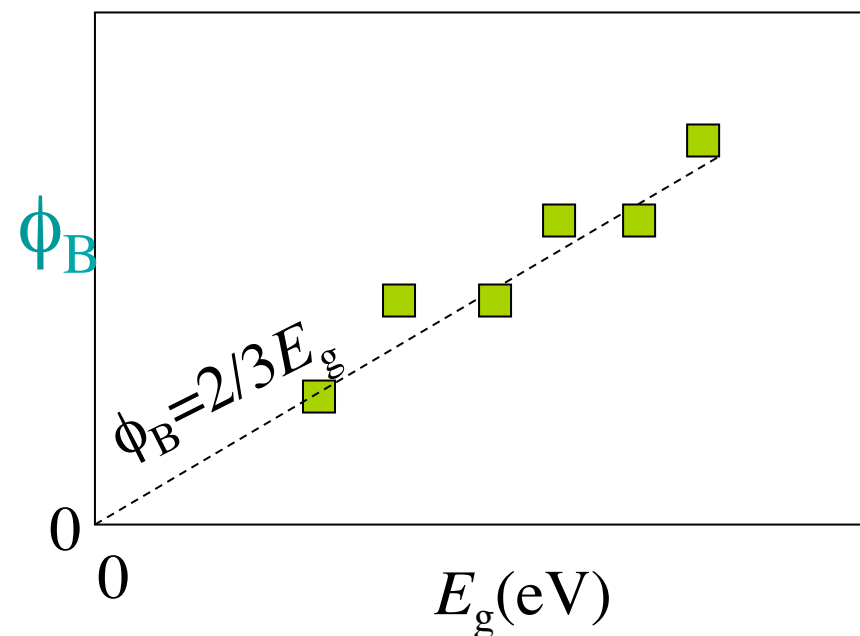
The experimental measurements

Schematic: ϕ_B for different metals on Si and GaAs

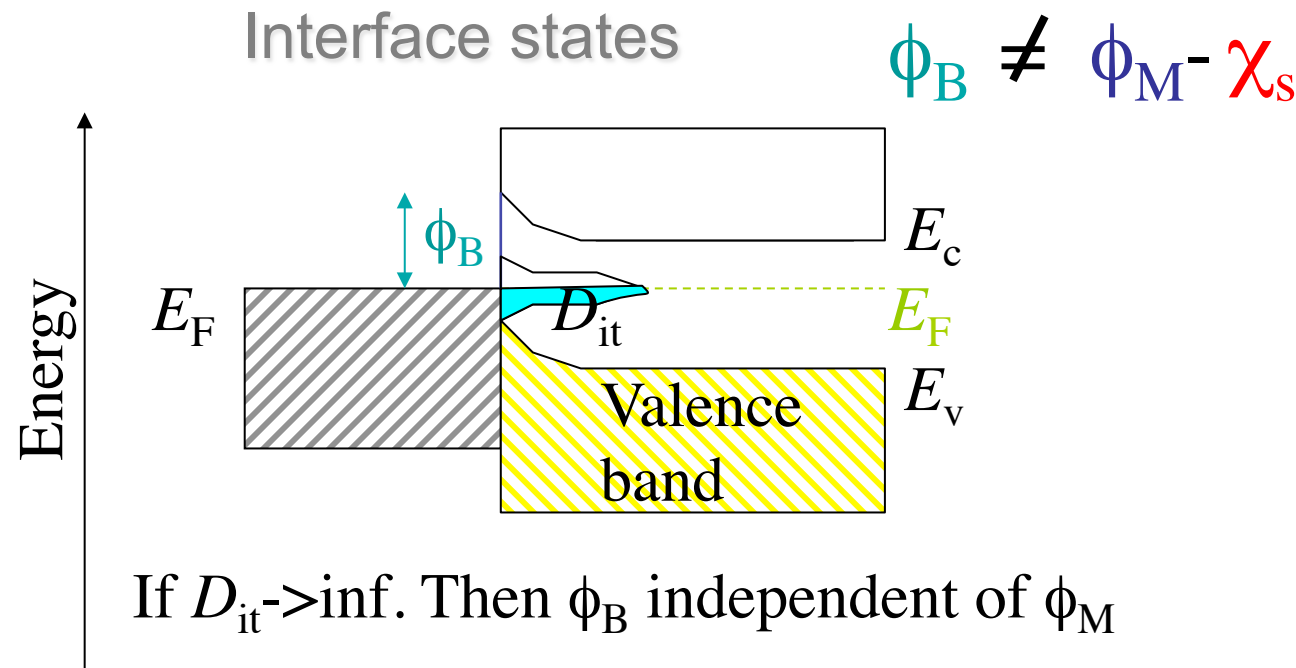


ϕ_B varies much more weakly with ϕ_M than the Shockley's equation

Schematic: ϕ_B for different semiconductors for Au metal



ϕ_B varies as rule of thumb $2/3 E_g$



High D_{it} will ‘pin’ the Fermi level at the interface

Why D_{it} , different origins, concepts, theoretical treatments

Tamm states

Heine states

MIGS states

Defects, dangling bonds, contamination

Metal/Semiconductor junctions

MIGS, metal induced gap states

Some characteristics according to Jerry Tersoff, PRL **52**, 465 (1984)

‘The defect model is itself defect’*

MIG: LDOS 0.02 states/atom eV \Rightarrow 0.3 nm screening length (a_{TF})

$$\phi_B = \frac{\text{Boundary dipole}}{\Delta\text{electroneg}} + \frac{\text{Dipole screened by MIGS}}{\text{bonding}} + \frac{\text{Charge neutrality}}{\text{Charge neutrality}}$$

If MIGS penetrate shallow \Rightarrow Boundary dipole dominates

If MIGS penetrate deep \Rightarrow ϕ_B varies little with el negativity

Surface: A few states is enough to pin E_F (defects or intrinsic states)

Screening length \sim 10-100 nm (depends on N_D)

\Rightarrow large dipole \Rightarrow E_F changes (charge neutrality)

Metal/Semicond: MIGS will screen all defects

*Measurements(partial metal coverage) do not represent metal/semicond Schottky barrier

Metal/Semiconductor junctions

‘The defect model’

- history

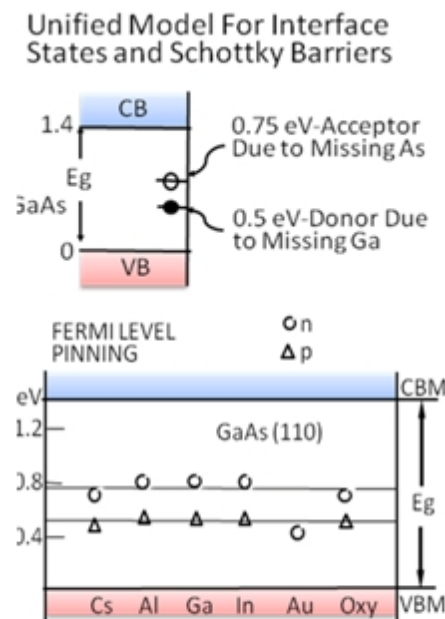


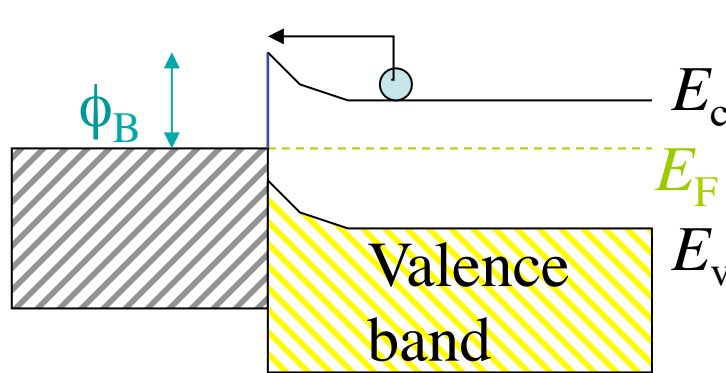
Fig. 6: Unified Defect Model by Spicer. [4] Left figure shows the defect levels of several cleaved semiconductor and Right figure shows the Fermi pinning levels for thin metal layer deposited on the Semiconductors.

Spicer's Defect Model

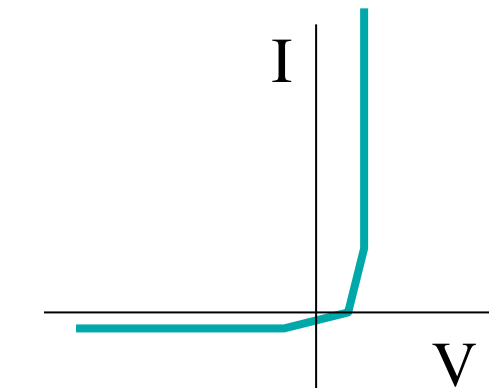
Spicer [4] claimed that the surface states created by dangling bond of covalent semiconductor is the major reason for Fermi level pinning observed at the MS junction. He deposited only few monolayers of metals on the Semiconductors and measured the Fermi level of the film. Experimentally he showed the evidence for defect pinning of Fermi level (Fig 6.) on surfaces with submonolayer metal coverage. However the results of these experiments were inconsistent with bulk barrier height measurements. In his lab, few monolayers of metal were not successfully deposited uniformly, rather those are bunched up. And some of the metals he used do not show metallic behavior at the monolayer thickness. Furthermore, more rigorous calculations done by Louie et al. showed that the intrinsic surface states of semiconductor or so called defects were removed by interaction with metal atoms and new surface states appeared due to the presence of the metal.

[4] W.E. Spicer et al., "Unified Defect Model and Beyond," J. Vac. Sci. Tech. **17**, 1019 (1980).

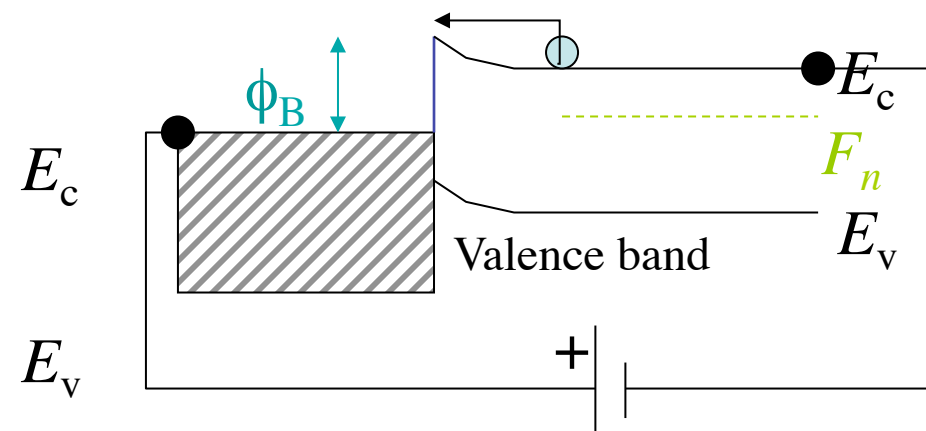
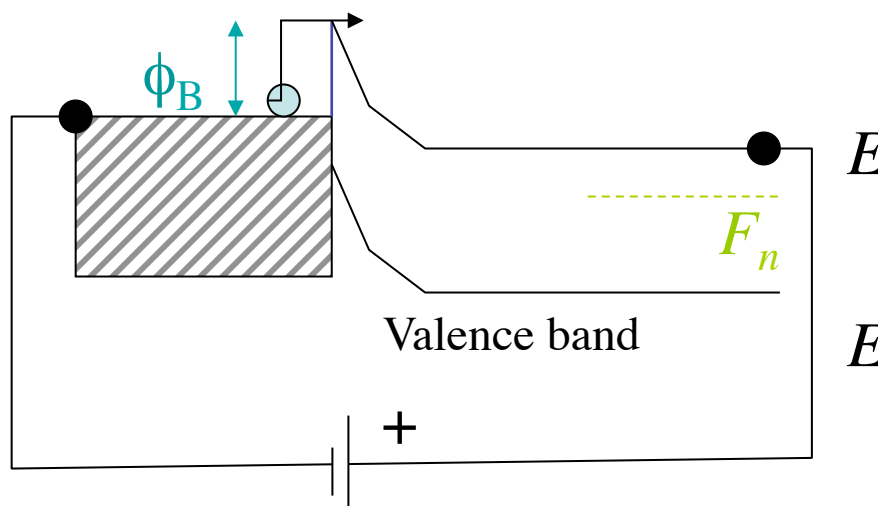
Current transport



Reverse bias



Forward bias



$$I = I_0 \left(\exp\left(\frac{qV}{kT}\right) - 1 \right)$$

$$I_0 = AA^{**} T^2 \exp\left(-\frac{\phi_B}{kT}\right)$$

Richardsons 'constant'

Idealized,
simplified
Thermionic model

Current transport2

$$I = I_0 \left(\exp\left(\frac{qV}{nkT}\right) - 1 \right)$$

n : ideality factor, 1.05, 2, 4
 How well the transport matches the idealizations/simplification of a model

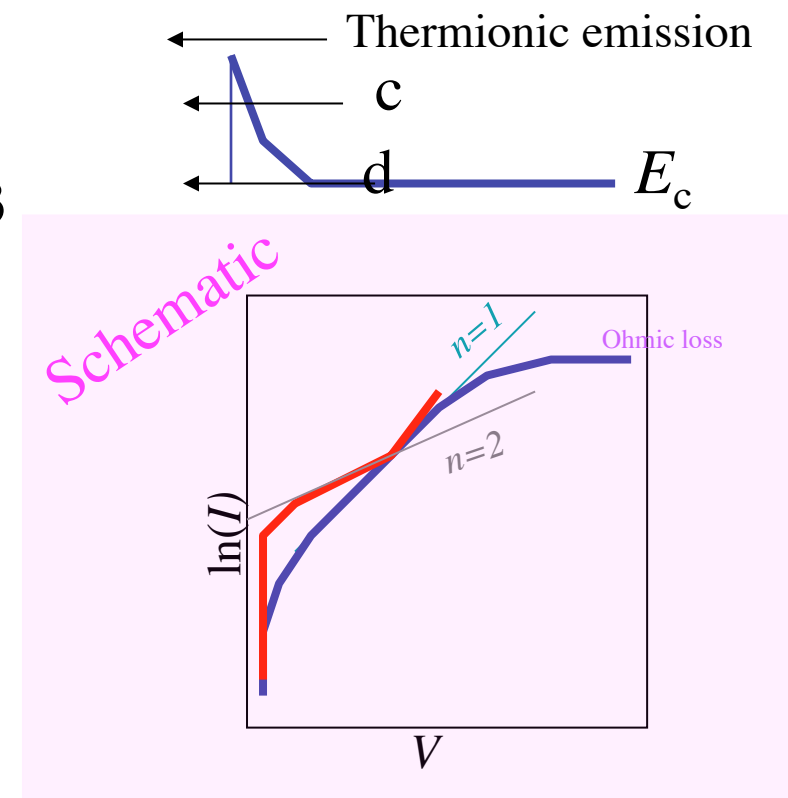
Reasons why not $n=1$

a Mirror image lowering $n \sim 1.04$

c Thermionic field emission $n \sim 1..3$

d Field emission (tunneling) $n > 4$

Recombination, $n=2$



Measure ϕ_B

I-V

$$I = I_0 \left(\exp\left(\frac{qV}{nkT}\right) - 1 \right) \quad I_0 = AA^{**} T^2 \exp\left(-\frac{\phi_B}{kT}\right)$$

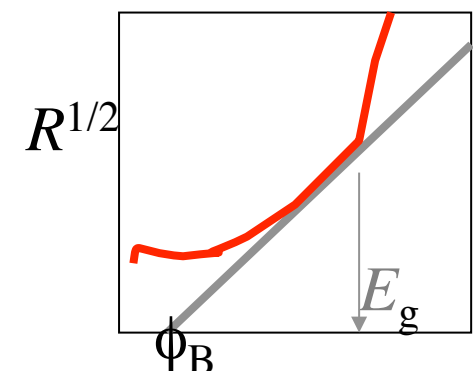
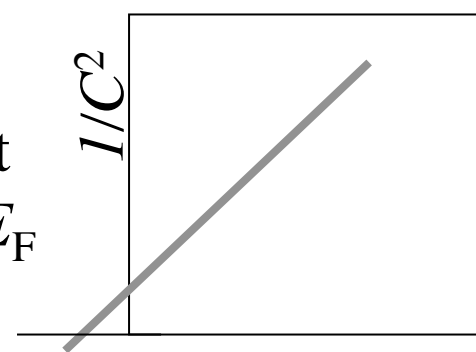
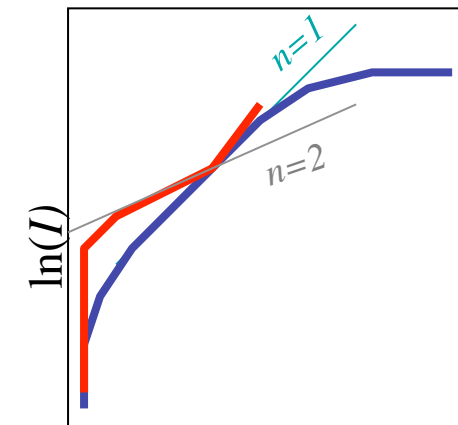
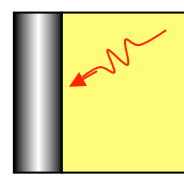
Measure I - V , determine I_0 , from intercept,
know $A, A^{**}(120)$

$$\text{C-V} \quad C = \frac{\epsilon_0 K_s A}{d} \quad d = \sqrt{\frac{\epsilon_0 K_s (\phi_B - E_c + E_F - V)}{q N_d}}$$

Measure CV , determine, ϕ_B - $(E_c$ - $E_F)$ from intercept
of V vs. $1/C^2$. Determine N_d from slope, Calc E_c - E_F
from N_d , N_d is measured from the slope

R vs. $h\nu$, Internal photo emission

Measure Response R vs. $h\nu, \phi_B$ from intercept
of $R^{1/2}$ vs. $h\nu$.





Ω -ic contacts

If all metal-1/2 cond junctions are rectifying
how can we make an ohmic contact?

- and what is an ohmic contact?

Characteristics for an ideal Ohmic contact:
can maintain equilibrium carrier concentration for all currents
flowing. (Infinite recombination velocity, perfect sink)
The voltage drop in the contact should be zero.

Ω -ic contacts

If all metal-1/2 cond junctions are rectifying
how can we make an Ohmic contact?

- and what is an Ohmic contact?

Characteristics for an ideal Ohmic contact:

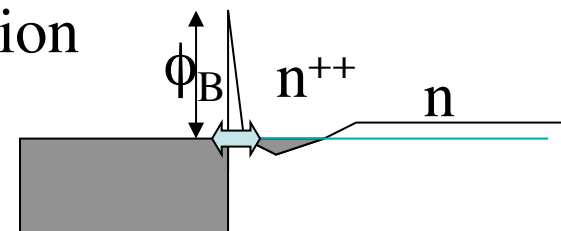
can maintain equilibrium carrier concentration for all currents flowing. (Infinite recombination velocity, perfect sink)

The voltage drop in the contact should be zero.

It is not possible to pick a metal with the ‘right’ ϕ_M ,?

Questionable approach because of interface states

Tunneling and high doping is the practical solution

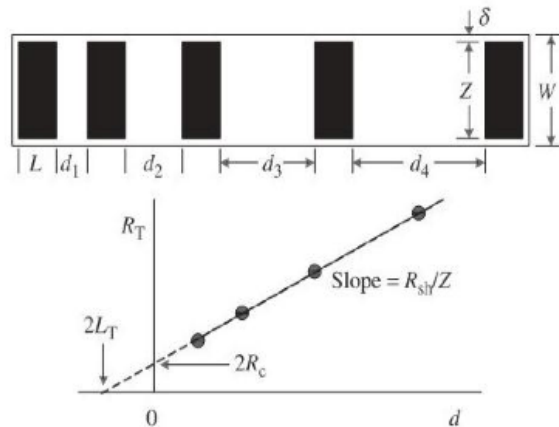


The high doping can be created by I^2 or in contact alloying or both

Ω -ic contacts

CONTACT RESISTANCE MEASUREMENT

Transfer length method



$$R_T = \frac{R_{sh}d}{Z} + 2R_c \approx \frac{R_{sh}}{Z}(d + 2L_T)$$

$$R_c = \frac{\rho_c}{LZ}$$

Fig. 3.22 A transfer length method test structure and a plot of total resistance as a function of contact spacing, d . Typical values might be: $L = 50 \mu\text{m}$, $W = 100 \mu\text{m}$, $Z-W = 5 \mu\text{m}$ (should be as small as possible), $d \approx 5$ to $50 \mu\text{m}$.

Specific contact resistivity can be obtained

- by interpolation...

Assumes identical sheet resistance under the contact

More complicated equations and specific contact resistivity required additional measurement

Ω -ic contacts

CONTACT RESISTANCE DEFINITIONS

What is R_c

Specific interfacial resistivity ρ_i (ohm cm²)

Resistance of metal-semiconductor contact

Defined as dV/dI when both voltage and contact area are zero

Theoretical quantity

$$\rho_i = \frac{\partial V}{\partial J} \Big|_{V=0}$$

$$\rho_i = \frac{\partial V}{\partial J} \Big|_{A \rightarrow 0}$$

Specific contact resistivity ρ_c (ohm cm²)

Includes a part of metal immediately above the contact and semiconductor below it

current crowding and no idealities of the interface

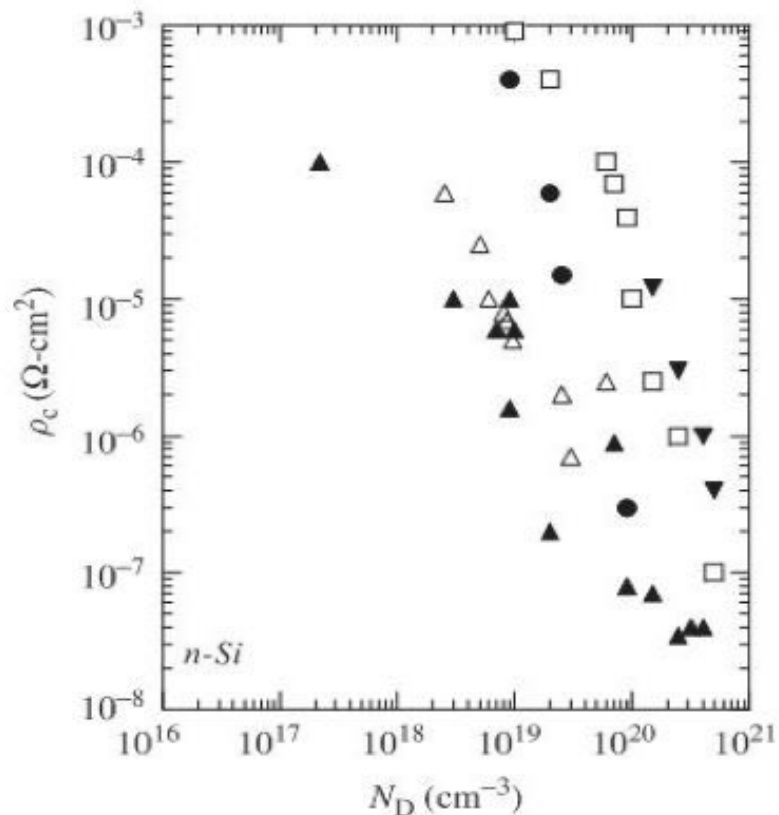
Independent of contact area

This is used

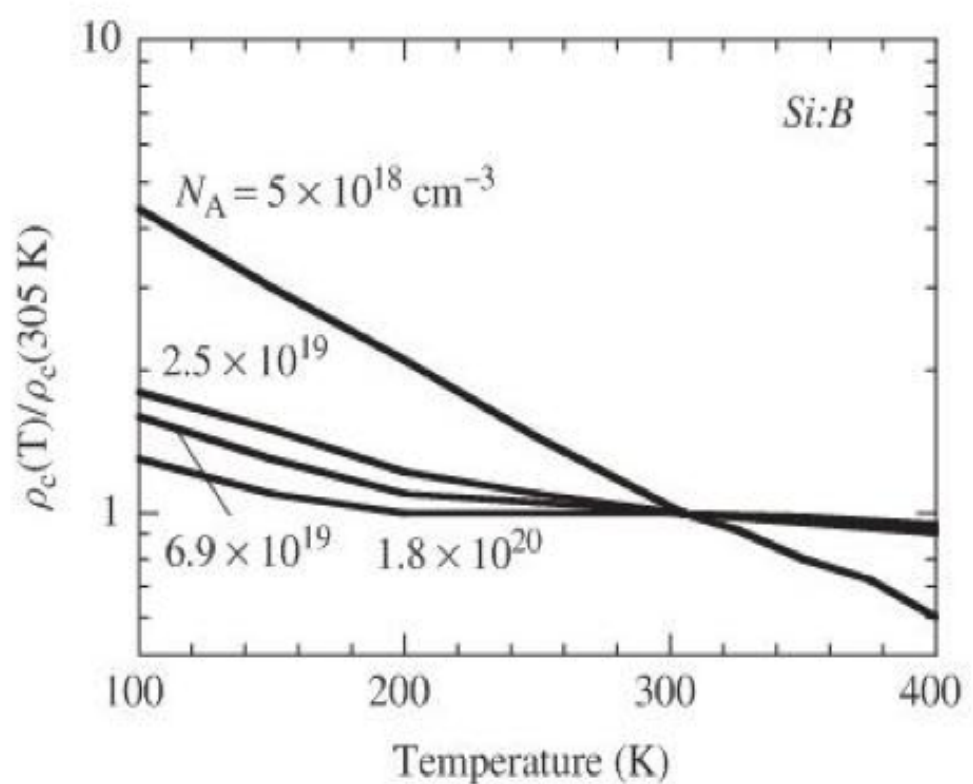
$$\rho_c = A_c R_c$$

Ω -ic contacts

CONTACT RESISTANCE DEPENDENCIES



Specific contact resistivity
versus doping density



Specific contact resistivity as a
function of temperature



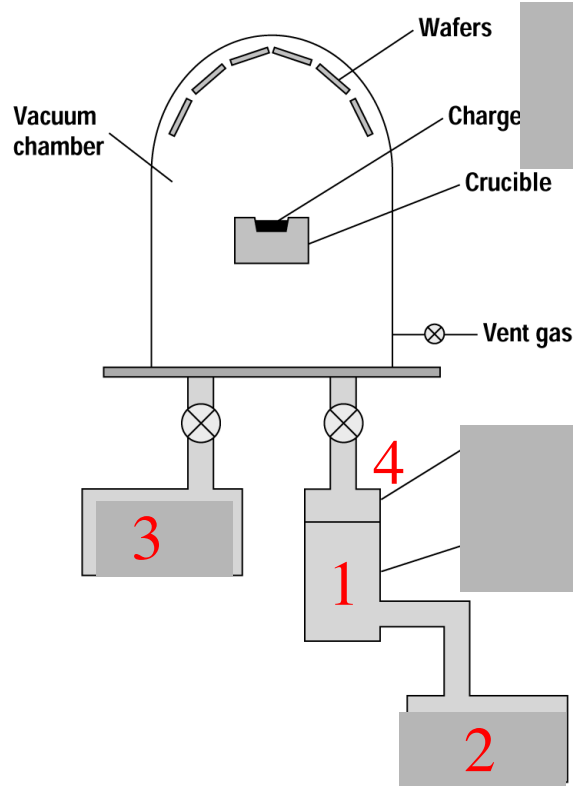
Metal film preparation

Methods, resulting structure

Evaporation - resistive heating, e-gun heating,
Sputtering, (laser ablation), CVD

Resulting structure - poly crystal metal film w grain boundaries

grain boundary diffusion different than bulk



Simplest evaporation by
resistive heating of metals

Figure 12.1 A simple diffusion-pumped evaporator showing vacuum plumbing and the location of the charge-containing crucible and the wafers.

Guess/recall from last week

Which kind of pumps are used here?

1 , 2 ,3

4 What is is this? It's function

Resistive boat

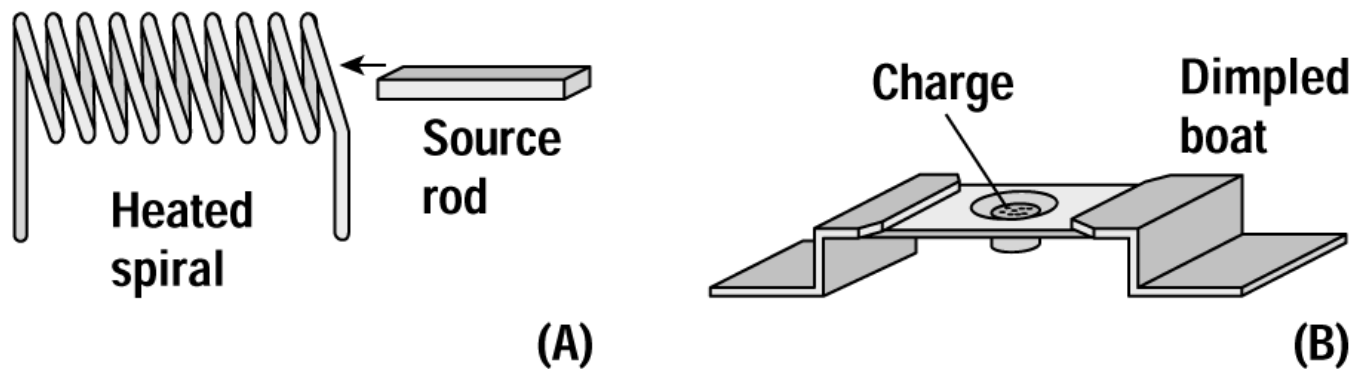


Figure 12.6 Resistive evaporator sources. (A) Simple sources including heating the charge itself and using a coil of refractory metal heater coil and a charge rod. (B) More standard thermal sources including a dimpled boat in a resistive media.

BN boat

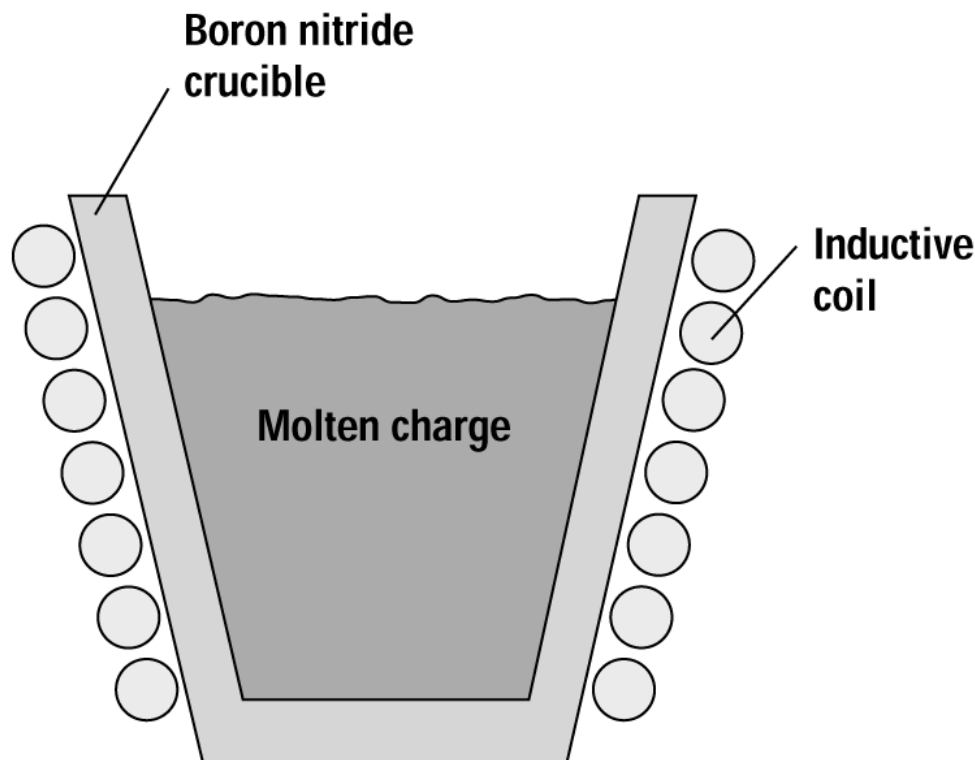


Figure 12.7 Example of an inductively heated crucible used to create moderately charged temperatures.

Vapor pressure of metals

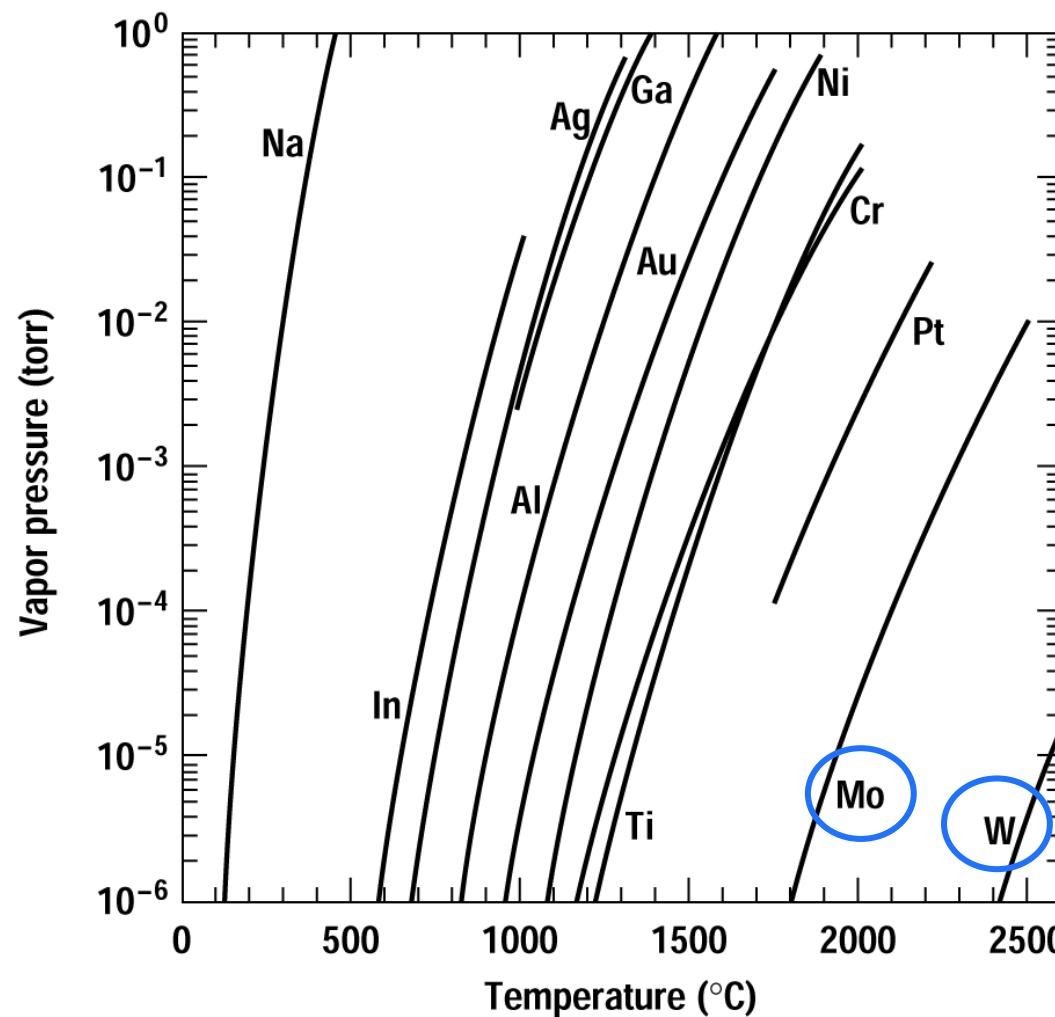


Figure 12.2 Vapor pressure curves for some commonly evaporated materials (*data adapted from Alcock et al.*).

E-gun, evaporation source

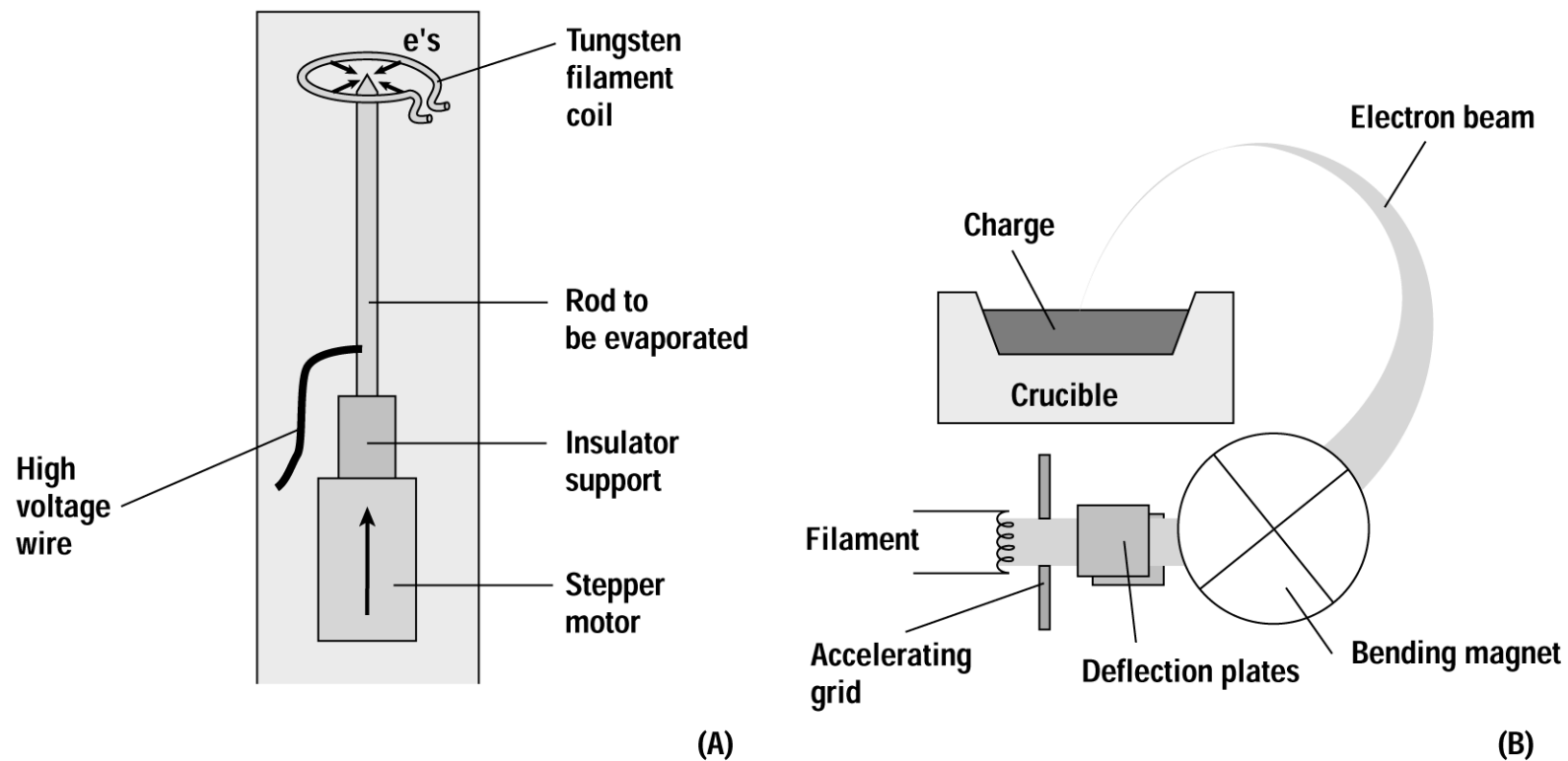


Figure 12.8 Electron beam evaporative sources. (A) A simple low-flux source using a hot wire electron source and a thin movable rod. (B) A popular source using a 270° source arc in which the beam can be rastered across the surface of the charge. The magnet must be much larger than shown to achieve the full 270° of arc.

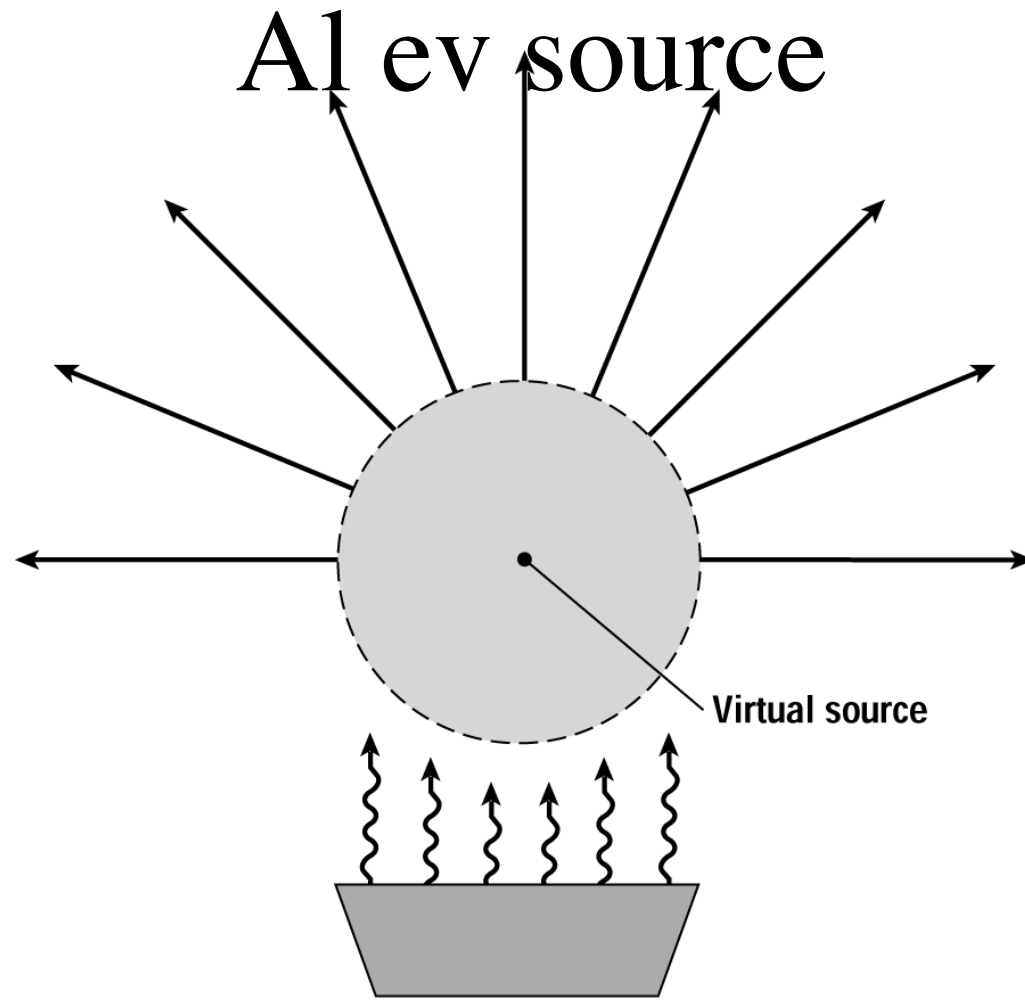


Figure 12.4 At high deposition rates, the equilibrium vapor pressure of the charge puts the region just above the crucible into viscous flow, creating a virtual source up to 10 cm above the top of the crucible.

Sputtering proc

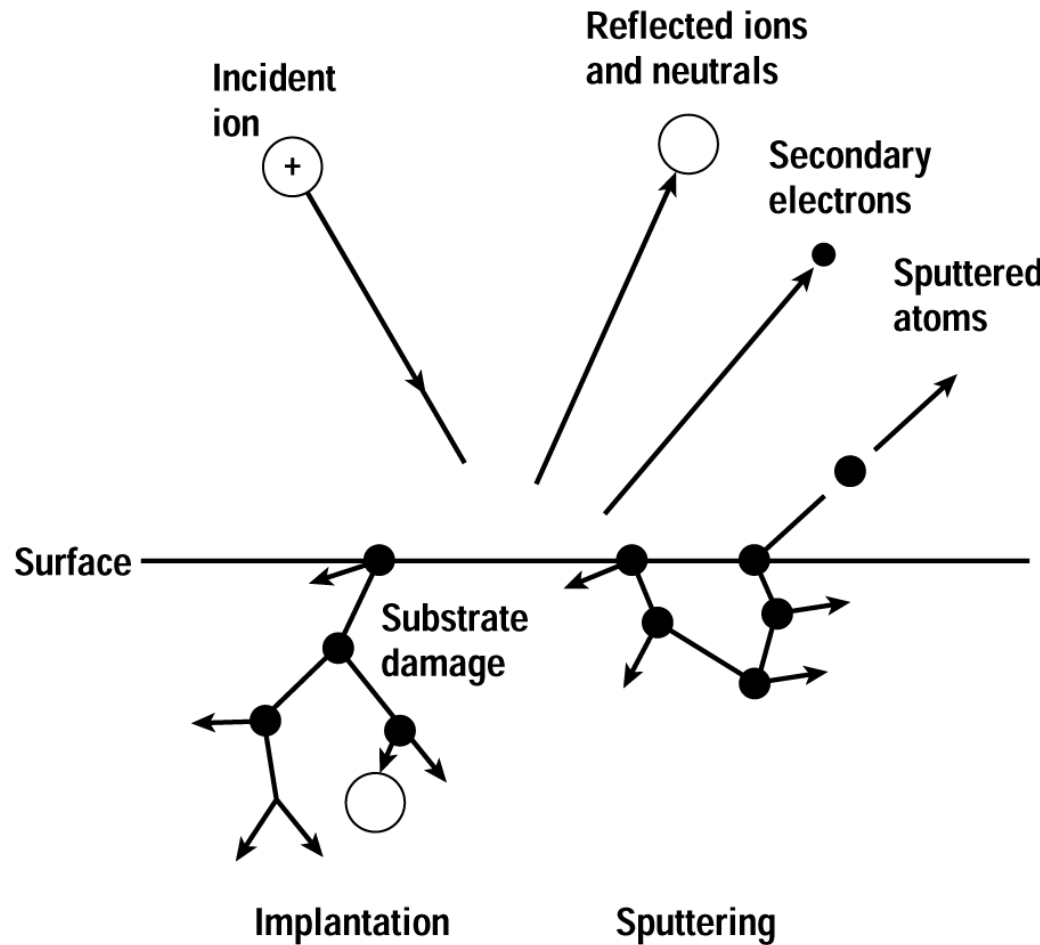


Figure 12.12 Possible outcomes for an ion incident on the surface of a wafer.

Magnetron sputter systems

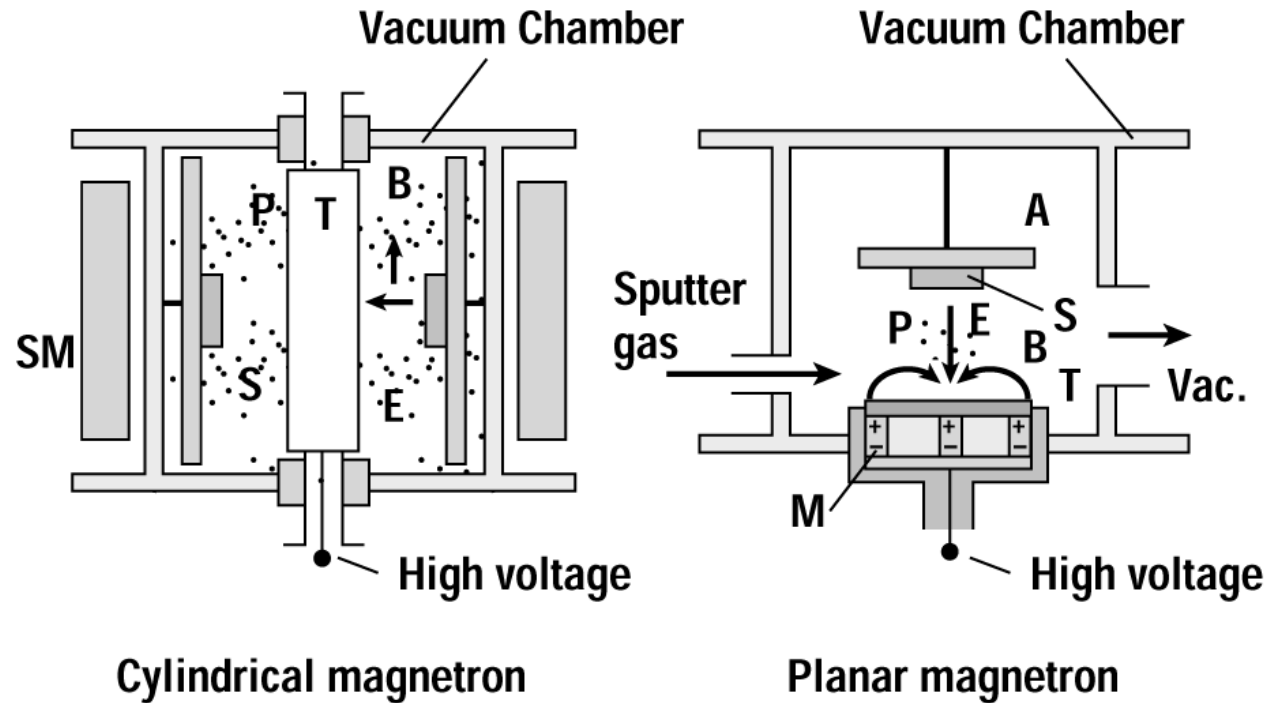


Figure 12.16 Planar and cylindrical magnetron sputtering systems T: target; P: plasma; SM: solenoid; M: magnet; E: electric field; B: magnetic field (*after Wasa and Hayakawa, reprinted by permission, Noyes Publications*).

Angle from source

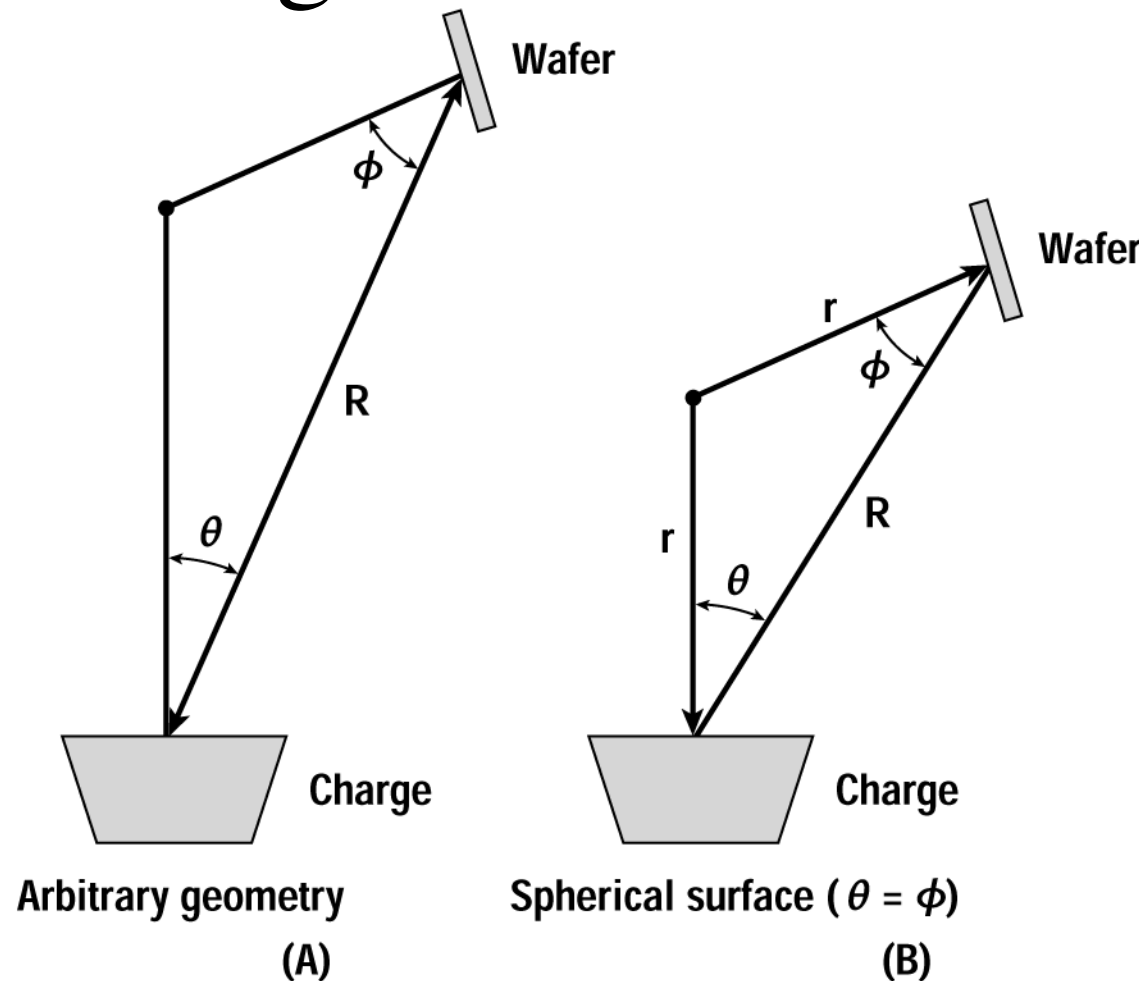


Figure 12.3 The geometry of deposition for a wafer (A) in an arbitrary position and (B) on the surface of a sphere.

Step coverage

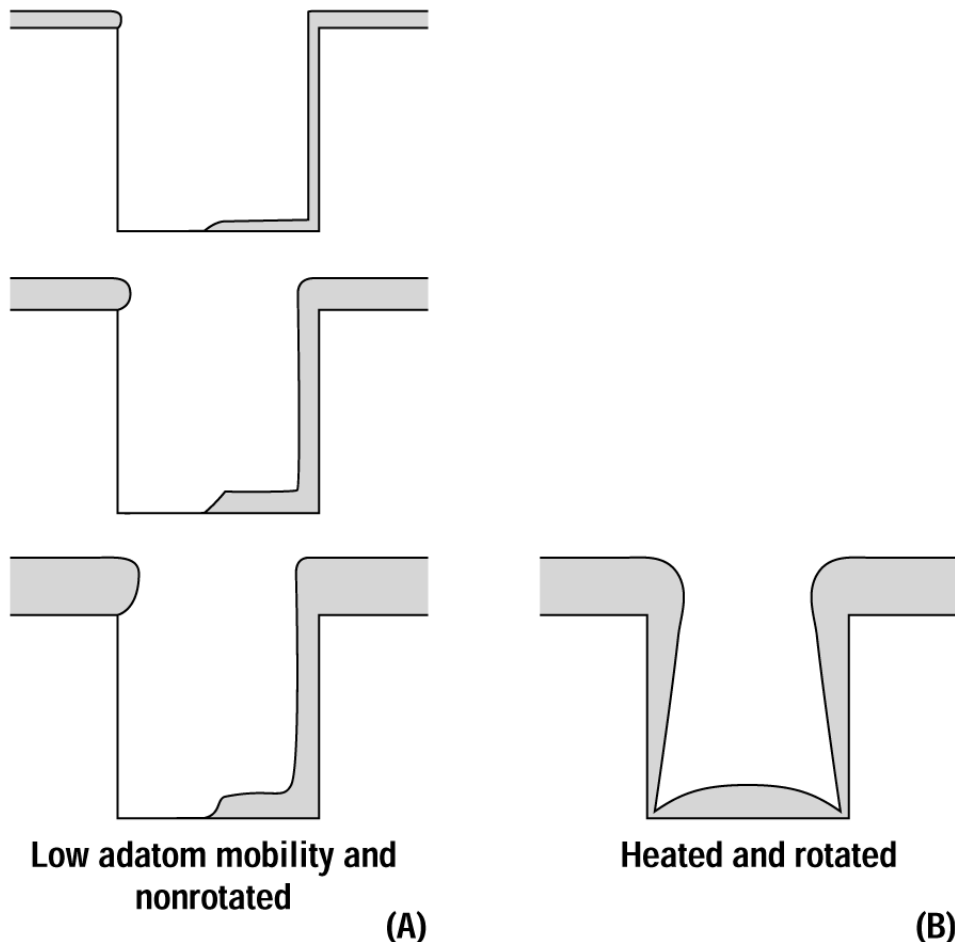


Figure 12.5 (A) Time evolution of the evaporative coating of a feature with aspect ratio of 1.0, with little surface atom mobility (i.e., low substrate temperature) and no rotation. (B) Final profile of deposition on rotated and heated substrates.

Step coverage

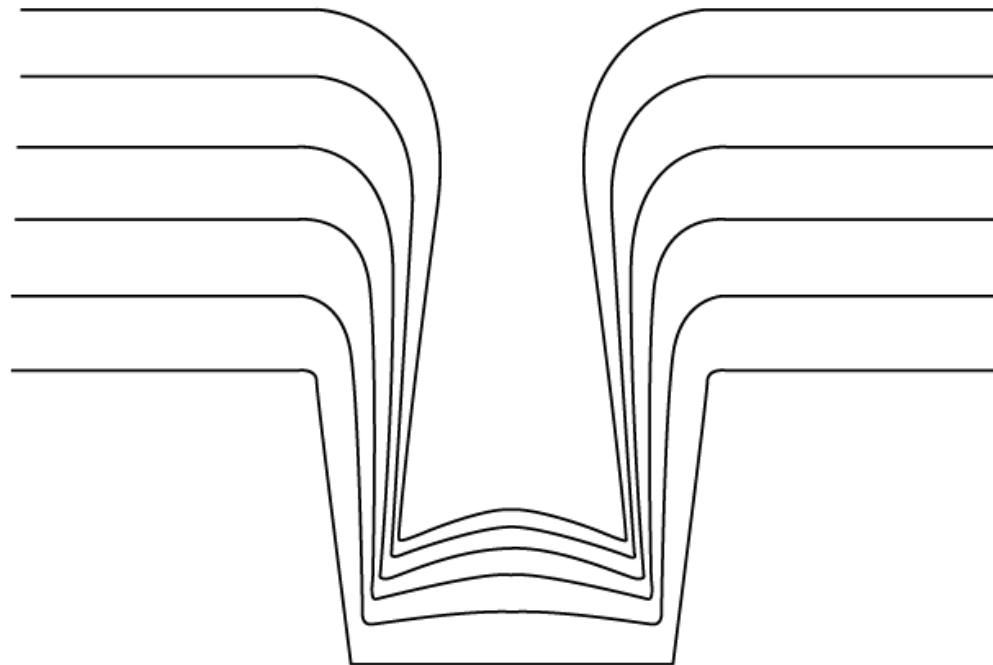


Figure 12.21 Cross section of the time evolution of the typical step coverage for unheated sputter deposition in a high aspect ratio contact.

PVD CVD system photo

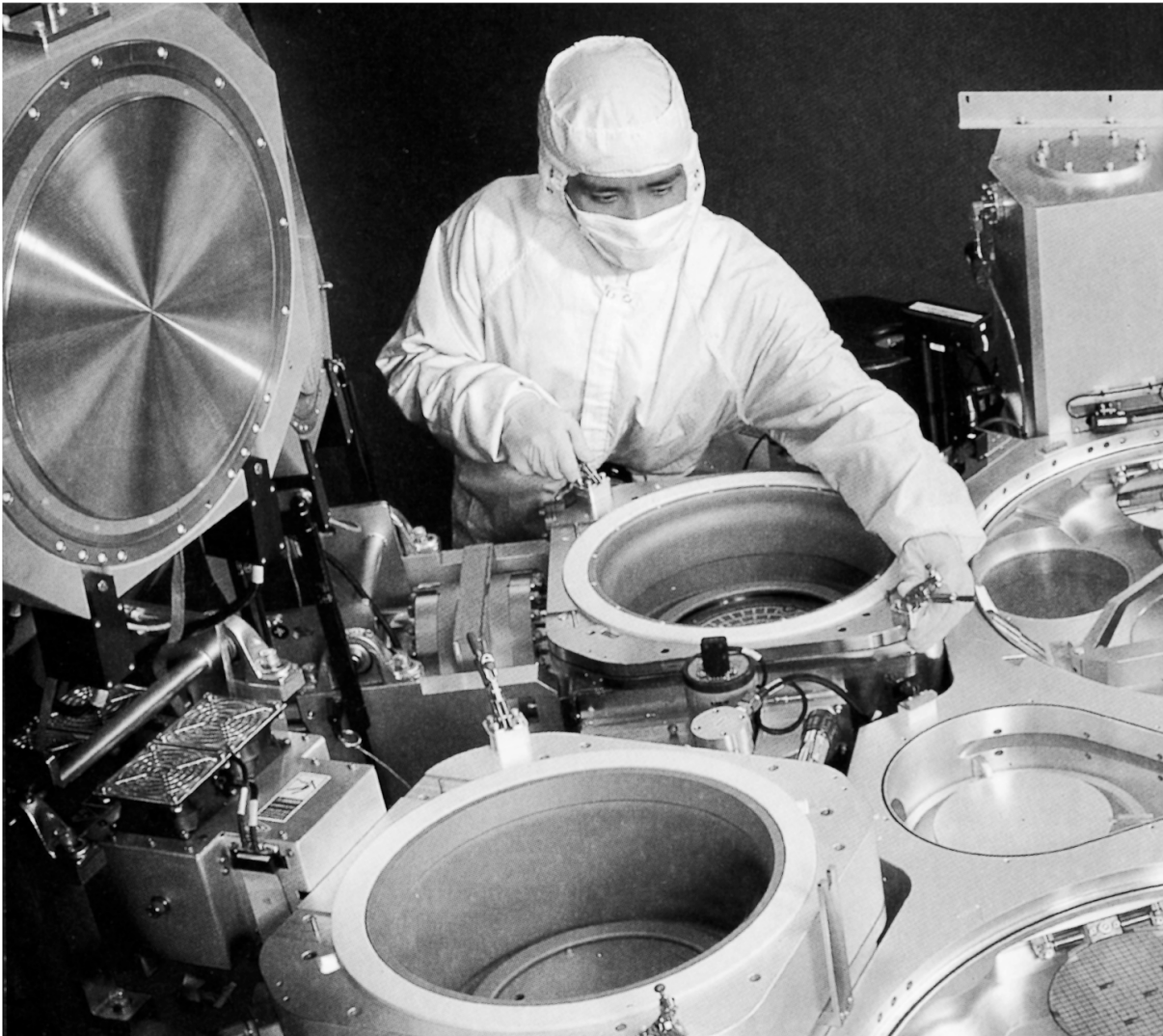
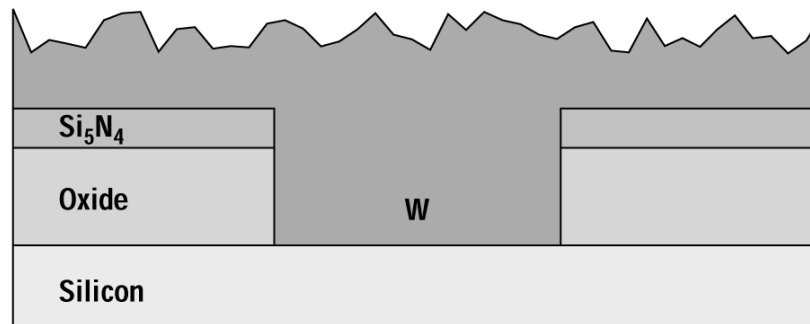
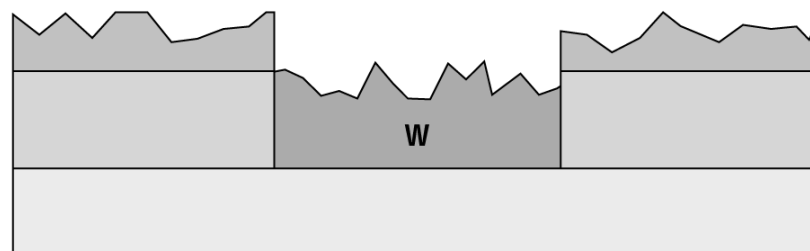


Figure 12.24 The Endura system by Applied Materials uses a number of PVD or CVD chambers fed by a central robot. For conventional and IMP sputtering, targets are hinged to open upward. Two open chambers are shown in this photograph along with the load lock (*from Applied Materials*).

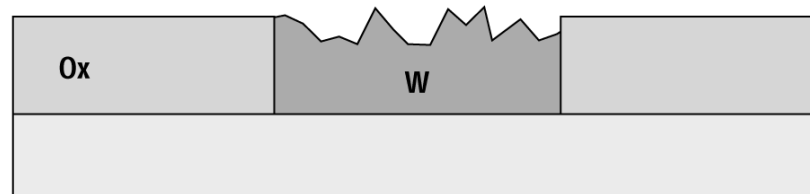
W CVD



(A)



(B)



(C)

Figure 13.24 The use of a sacrificial nitride layer with tungsten CVD to avoid surface roughening (*after Schmitz, ©1992, Noyes*).

Selective W deposition



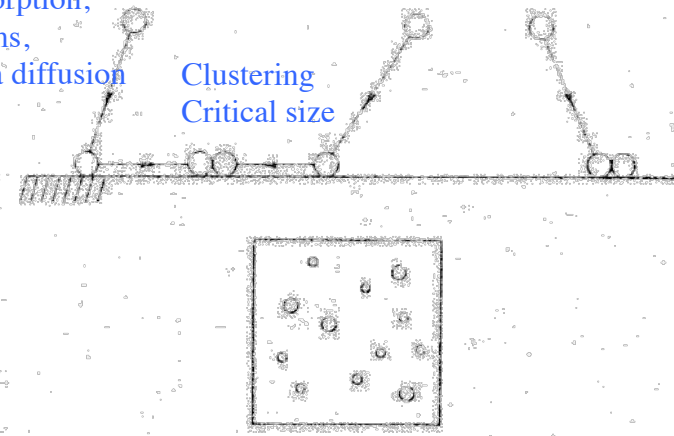
Figure 13.25 Damage to the substrate produced by selective tungsten.

Evolution of film structure

I. Generation of nuclei

Physisorption,
Adatoms,
Surfaca diffusion

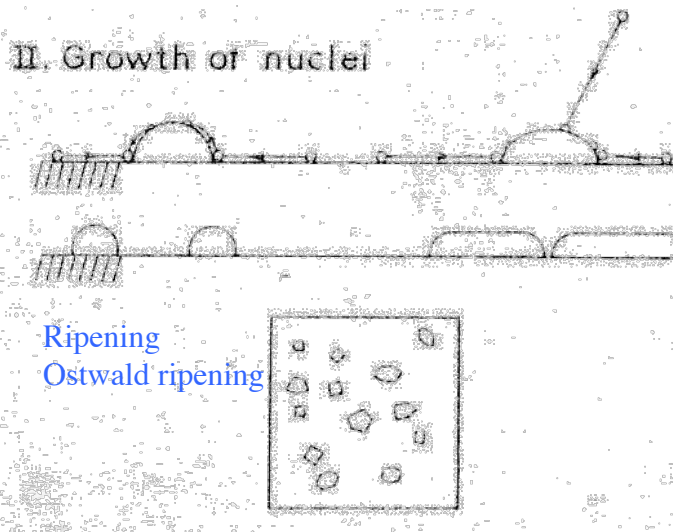
Clustering
Critical size



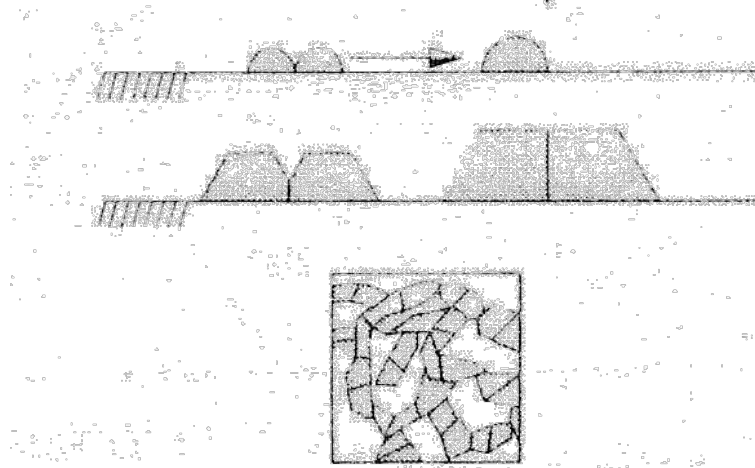
Frank-van der Merwe
Volmer-Weber
Stranski-Krastanov

II. Growth of nuclei

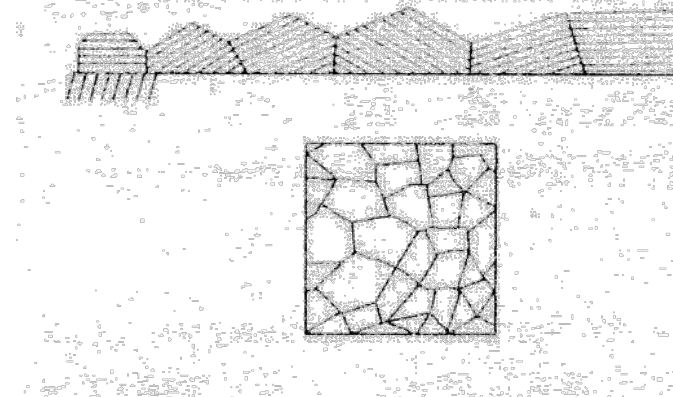
Ripening
Ostwald ripening



III. Contact and coalescence of metal particles

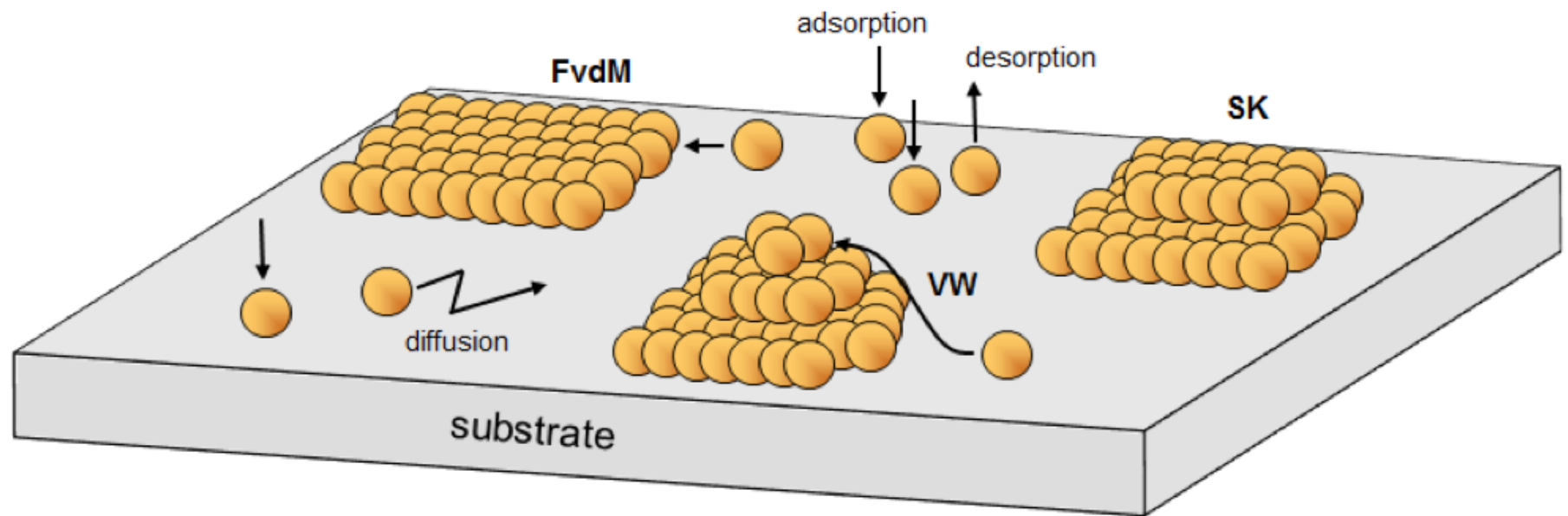


IV. Outgrowth of continuous layer



Growth stages of thin film metal films during deposition (weakly bound atoms)

Short reminder of the common growth mode of thin films – from epi growth



Frank-van der Merwe

Volmer Weber ←

Stranski Krastanov

Mostly consider this for non epi

Three Structure Zone Model

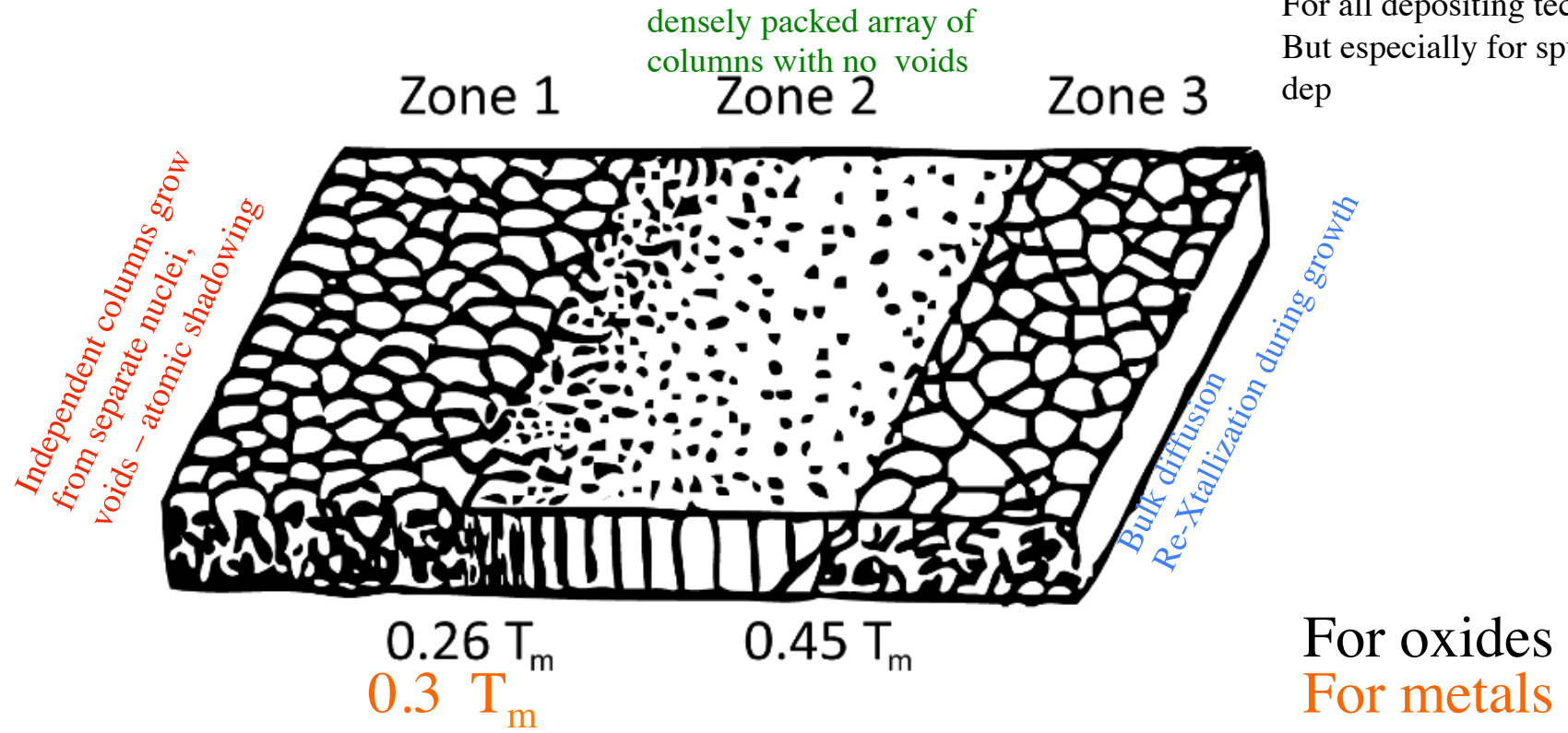


Figure 2.1: Movchan and Demchishin's structure zone model showing three distinct morphological zones in a thin film as temperature increases from left to right [12]. The transition temperatures are expressed as fractions of the material's melting point, and are given here for oxides [13]. Increasing temperature increases adatom diffusion, creating void-separated columns (Zone 1), densely-packed columns (Zone 2), and finally joined crystallites (Zone 3). Adapted from [12].

GLANCING ANGLE DEPOSITION

As an illustration of the independent column growth zone I

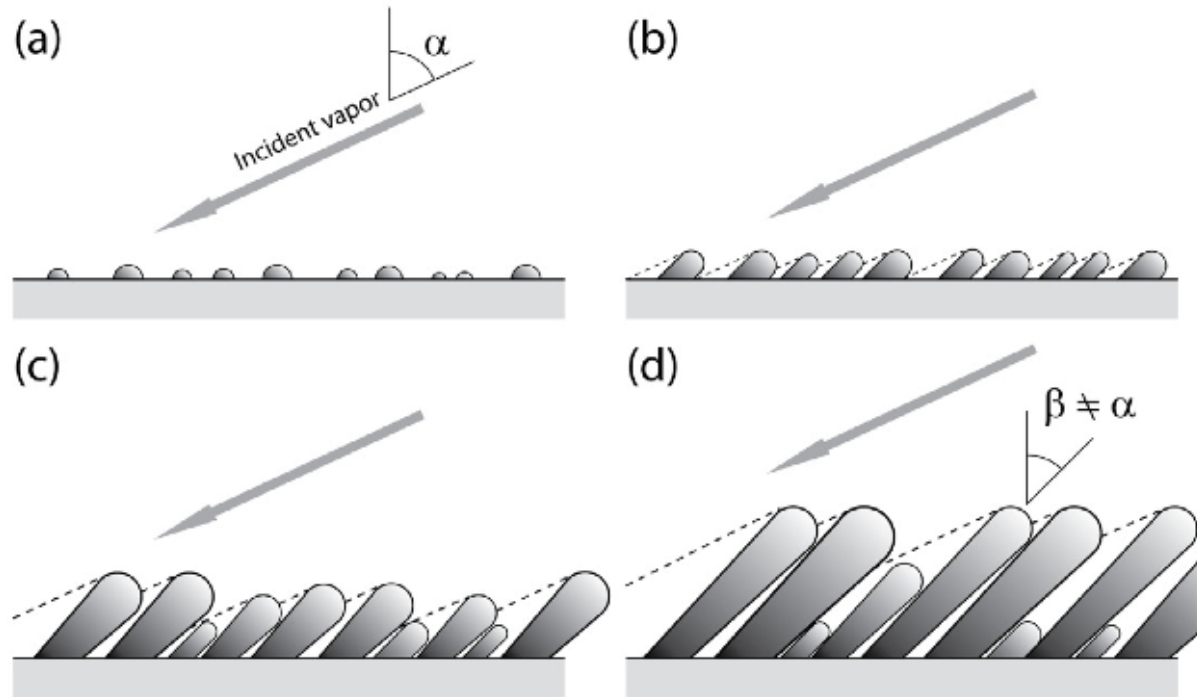
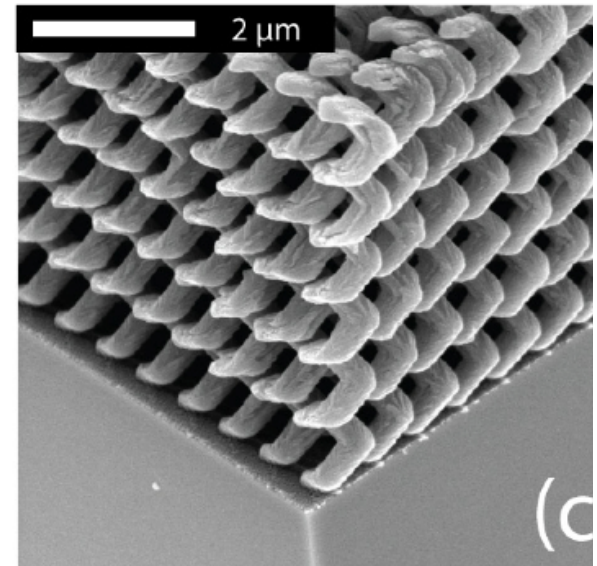
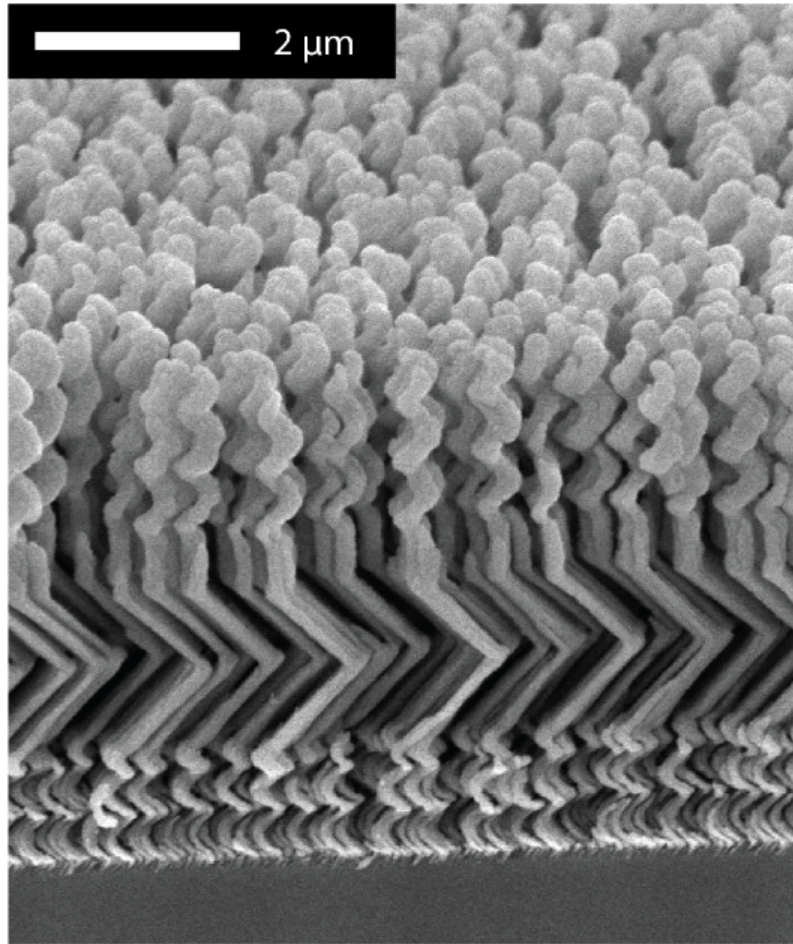


Figure 2.2: Diagram of the shadowing process at the heart of glancing angle deposition. Nuclei (a) that form in the early stages of growth shadow the regions behind them from the incoming flux, causing preferential growth into columns (b). As these grow, the shadowing process can starve slower-growing columns from flux entirely, causing column extinction (c). Columns bend toward the flux (d), but the angle of inclination β is less than the angle of incoming flux, α . Figure reproduced with permission from [20].

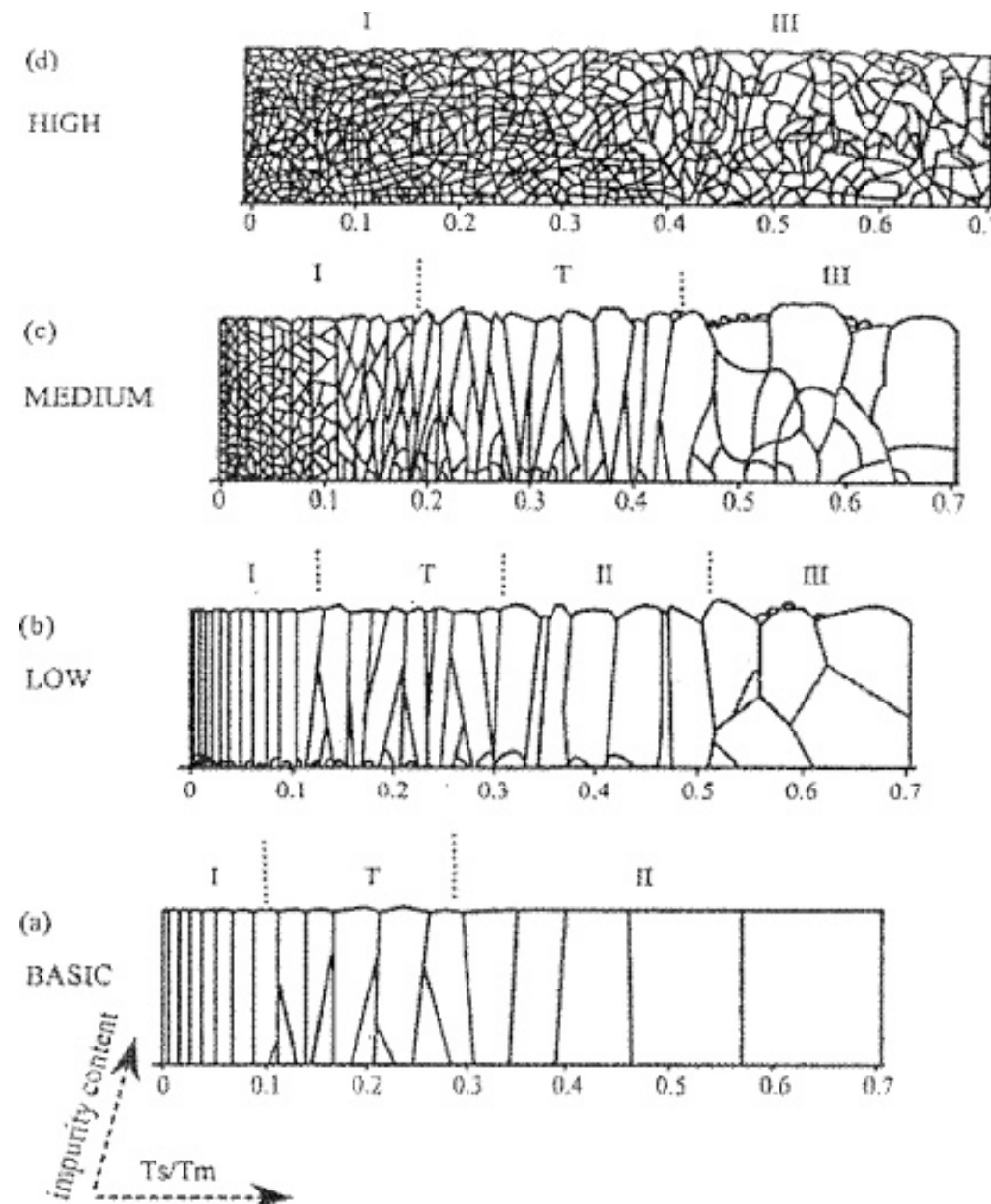
GLANCING ANGLE DEPOSITION

As an illustration of the independent column growth zone I



Film highlighting the breadth of control GLAD allows over nanostructure morphology. The film bottom has three turns of a right-handed TiO_2 helix, grown at 450 nm, followed by a SiO_2 zig-zag, a section of SiO_2 vertical post, and finally a left-handed SiO_2 helix. Figure taken with permission from [30].

EFFECT OF IMPURITY CONTENT on STRUCTURE of FILMS



Three zone model for sputter-dep.

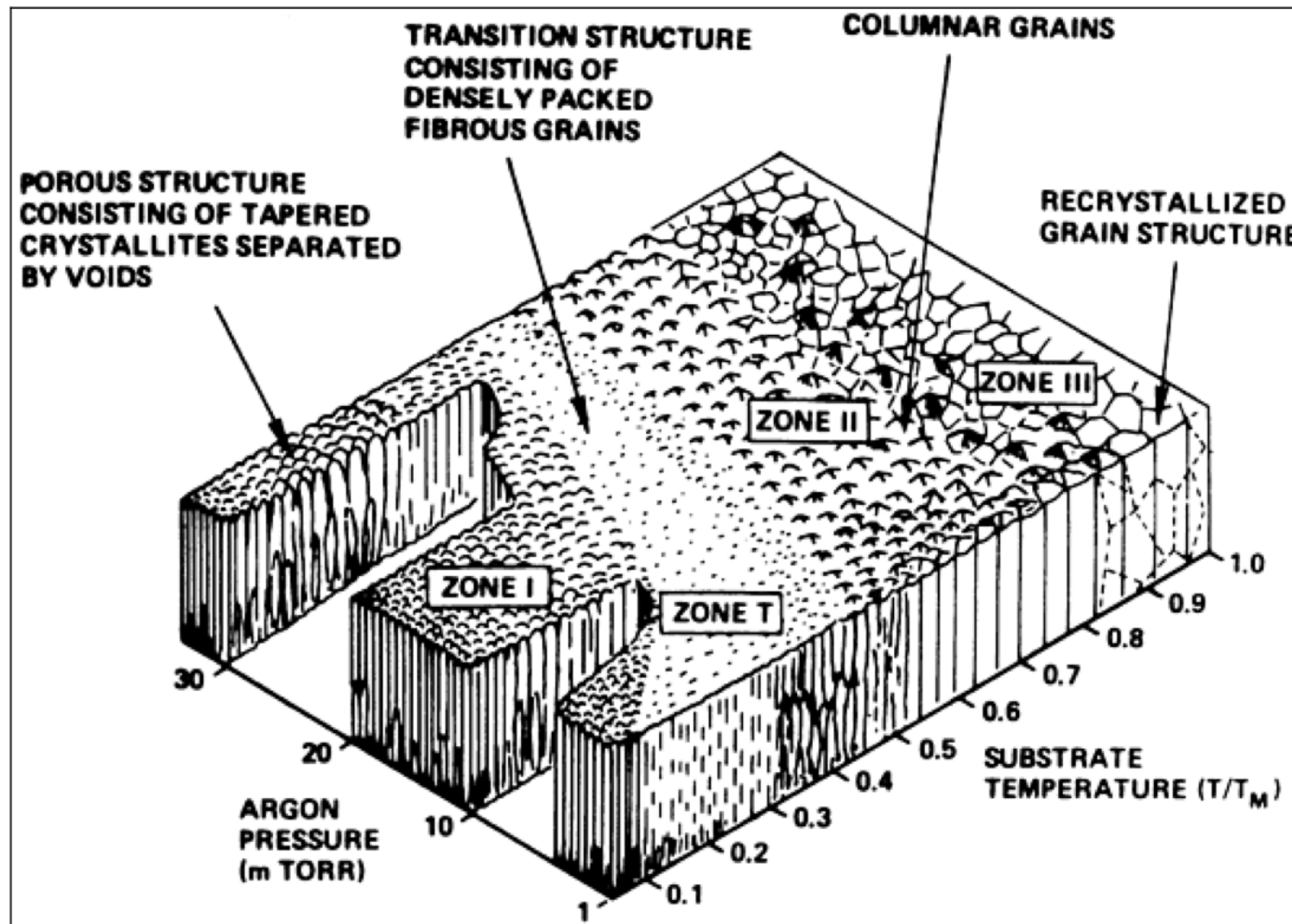


Fig. 4. Thornton zone model (Thornton, 1974)

Pressure influence kinetic energy of deposited atom,
Increasing pressure has same effect as decreasing temp

Stress in deposited films

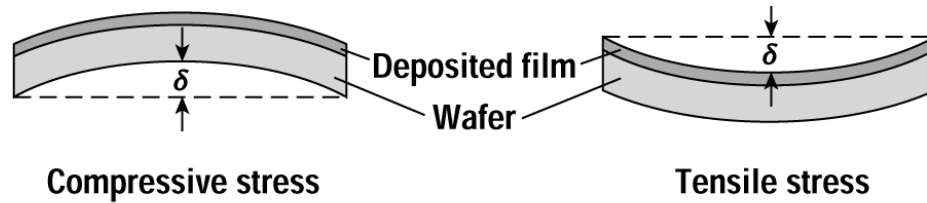


Figure 12.29 The change in wafer deflection may be used to measure the stress in a deposited layer. This is typically measured using a reflected laser beam.

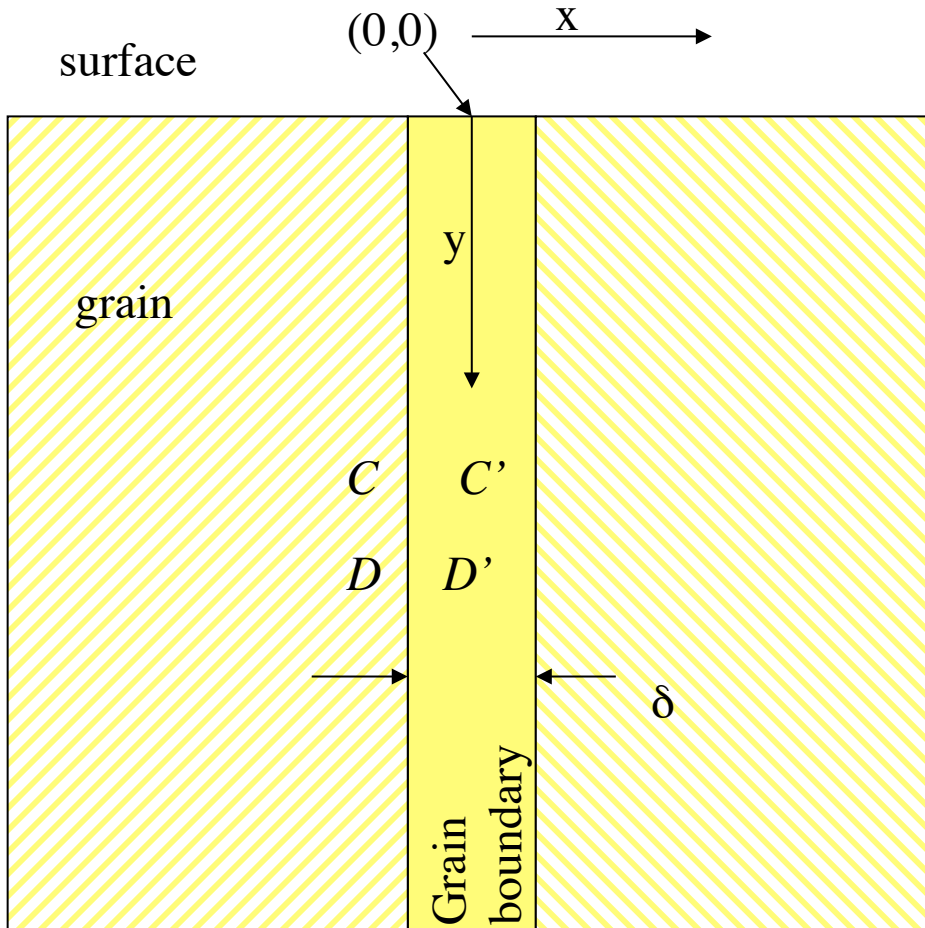
Reasons for stress

Deposition at high temperature -difference in thermal expansion

Internal stress

Grain boundary diffusion

important for growth of thin films, engineering of thin films



Fick's 1st

$$J = -D \frac{\partial C}{\partial x}$$

Cont. eq

$$\nabla J = \frac{\partial C}{\partial t}$$

Ficks 2nd

$$\frac{\partial C}{\partial x} = D \frac{\partial^2 C}{\partial x^2}$$

iff $\frac{\partial D}{\partial C} = 0$

The problem at hand is solution of Fick 2nd
Inside and outside of grain boundaries

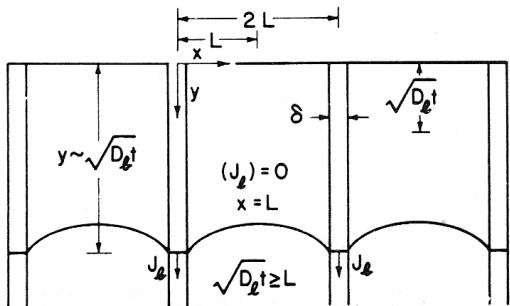
Continuity condition at grain boundary

$$C = C' \quad D \frac{\partial C}{\partial t} = D' \frac{\partial C'}{\partial t} \quad (J = J')$$

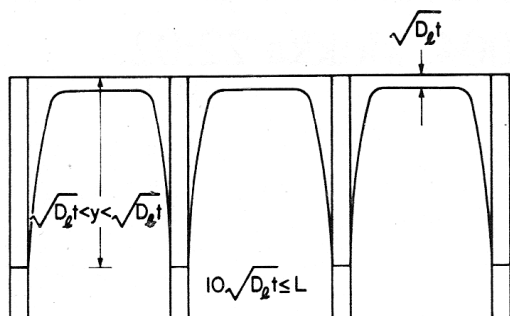
Appropriate conditions for free surface

Grain boundary diffusion

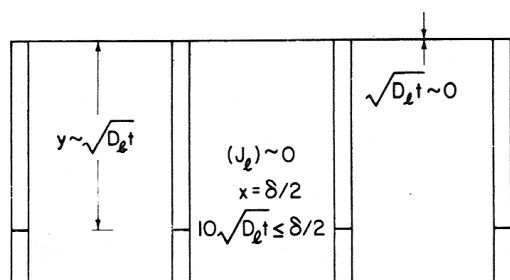
KINETICS - MODES



(a) A-KINETICS



(b) B-KINETICS



(c) C-KINETICS

Figure 7.1. Schematic representation of A-, B-, and C-kinetics. Vertical lines indicate grain boundaries, and curved lines are isoconcentration contours. The diffusion source coincides with the top horizontal lines.

Grain boundary diffusion, model Whipple, Fisher

Basic equations

$$\begin{aligned} \textcircled{1} \quad D' \nabla^2 C' &= \frac{\partial C'}{\partial t} ; \quad \text{grænsebet} \\ &\text{for } x = \pm \frac{\Delta}{2} \quad C' = C \\ \textcircled{2} \quad D \nabla^2 C &= \frac{\partial C}{\partial t} \\ &\text{for } y = 0 \quad C = C(x, 0, t) = 0 \quad \textcircled{4} \end{aligned}$$

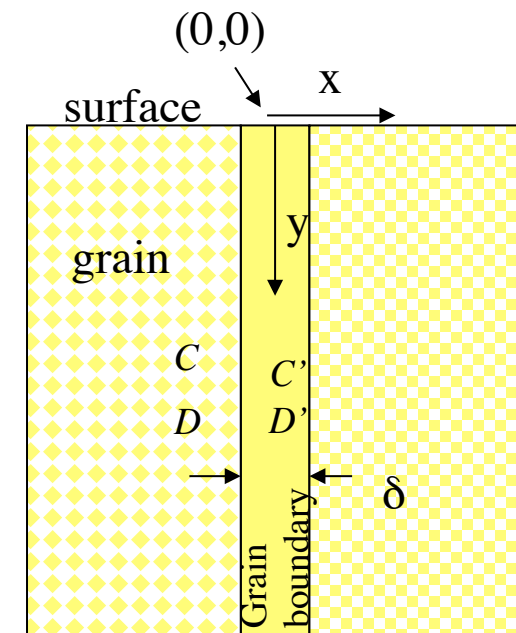
Expansion of C'

$$C'(x, y, t) = C_0'(y, t) + \frac{x^2}{2} C_2(y, t) \quad \textcircled{5}$$

$$\textcircled{5} \rightarrow \textcircled{1} \quad D' \left(\frac{\partial^2 C_0'}{\partial y^2} + C_2' \right) = \frac{\partial C_0'}{\partial t} \quad \textcircled{6}$$

$$\textcircled{3} \& \textcircled{4} \quad C \approx C_0' , \quad D \frac{\partial C}{\partial x} = D' \frac{\partial C_0'}{\partial x} \quad \textcircled{7}$$

$$\textcircled{7} \rightarrow \textcircled{6} \quad D' \frac{\partial^2 C}{\partial y^2} + \frac{D}{\delta/2} \frac{\partial C}{\partial x} = \frac{\partial C}{\partial t}$$



Solution by Fourier-Laplace transform

$$C = \operatorname{erfc} \frac{\eta}{2\sqrt{\pi}} + \frac{\eta}{2\sqrt{\pi}} \int_{-\infty}^{\Delta} \frac{dG}{G^{3/2}} \exp(-\frac{\eta^2}{4G}) \operatorname{erfc} \frac{1}{2} \sqrt{\frac{\Delta-1}{\Delta-6}} i$$

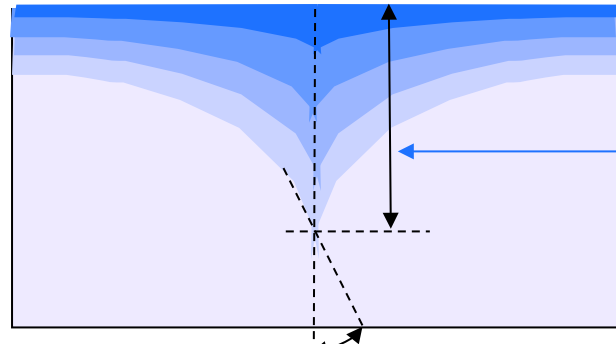
$$\xi = \frac{x-a}{\sqrt{Dt}}, \quad \eta = \frac{y}{\sqrt{Dt}}, \quad \beta = \left(\frac{D'}{D}-1\right) \frac{a}{\sqrt{Dt}}, \quad \Delta = \frac{D'}{D}$$

INPRACTICAL

Grain boundary diffusion, Le Claire model

Better suited for comparison with experiments

alternatives



1 Measure distance to apex

2 Measure angle

3 Measure average (lateral) concentration vs. depth

$$D'\delta = \left(\frac{\partial \ln \bar{c}}{\partial y} \right)^{-2} \left(\frac{4D}{t} \right)^{1/2} \left(\frac{\partial \ln \bar{c}}{\partial \eta \beta^{-1/2}} \right)$$

$$\beta = \frac{\left(\frac{D'}{D} - 1 \right) \delta}{2\sqrt{Dt}}$$

= LeClaire
diffusion parameter

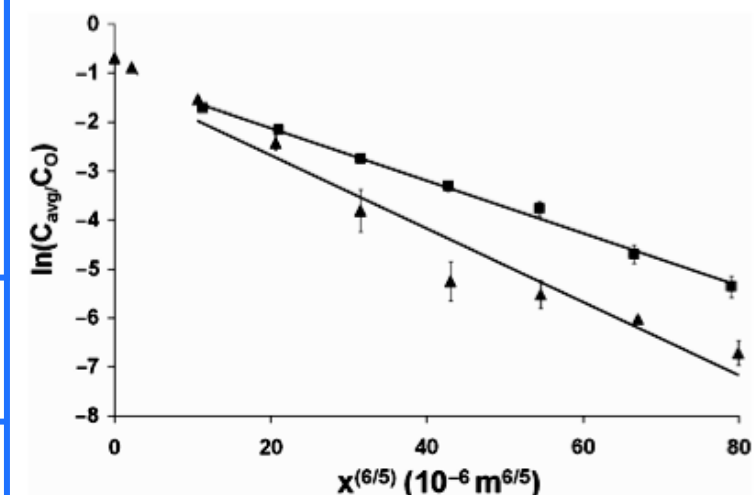
If β is big i.e. grain boundaries dominate

$$D'\delta = \underbrace{\left(\frac{\partial \ln \bar{c}}{\partial y^{6/5}} \right)^{-5/3}}_{\text{Can be measured}} \left(\frac{D}{t} \right)^{1/2} 1.32$$

D may be known

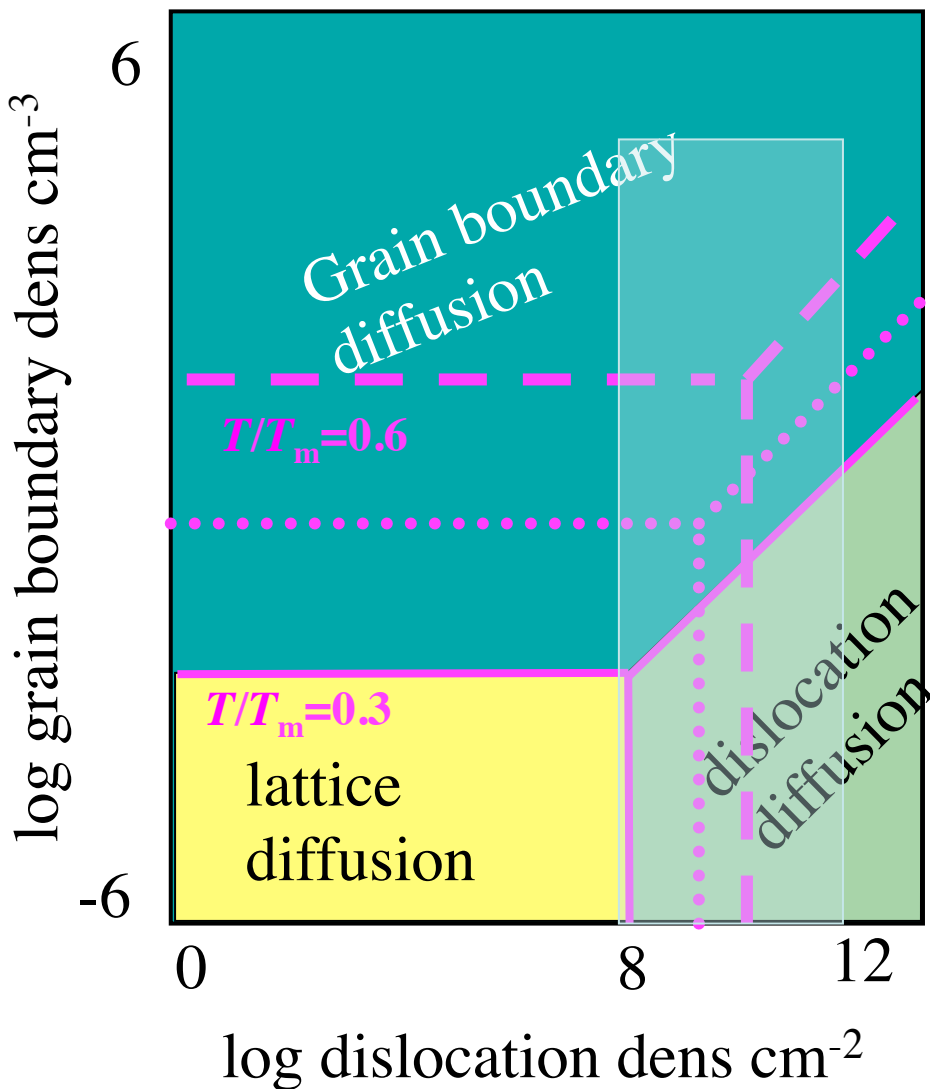
measures $D'\delta$

Plot $\ln \bar{c}$ vs. $y^{6/5}$



Grain boundary diffusion, dislocations and lattice diffusion

Regimes of dominance



Si-Al metallization

Al, wildly used metallization for Si
Due to many problems, other metals
Have taken over,
important to know if you work with Si

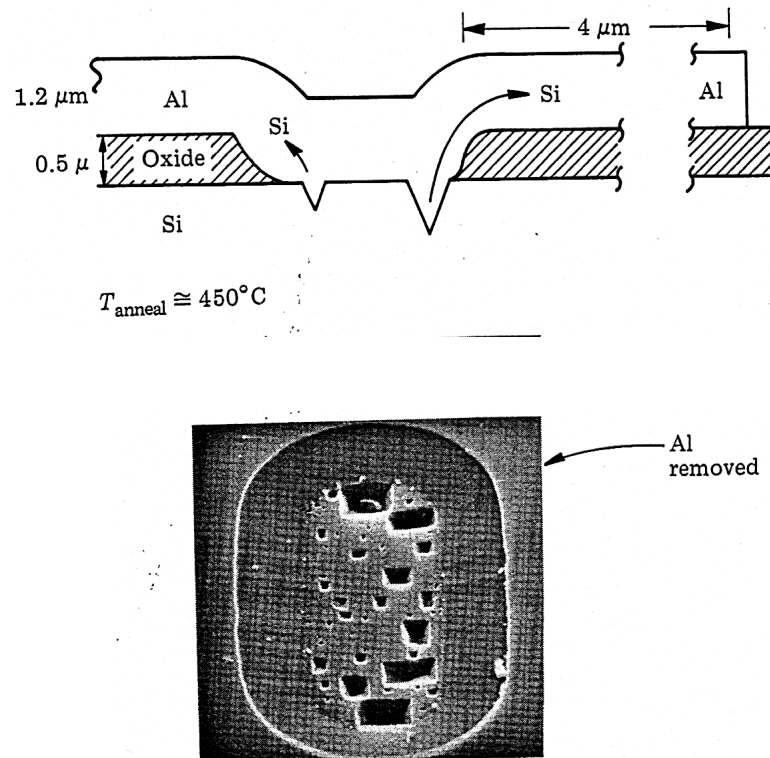


FIGURE 10.5 Pit formation of Al contact to Si.

Spikes,
short circuit ‘potential’

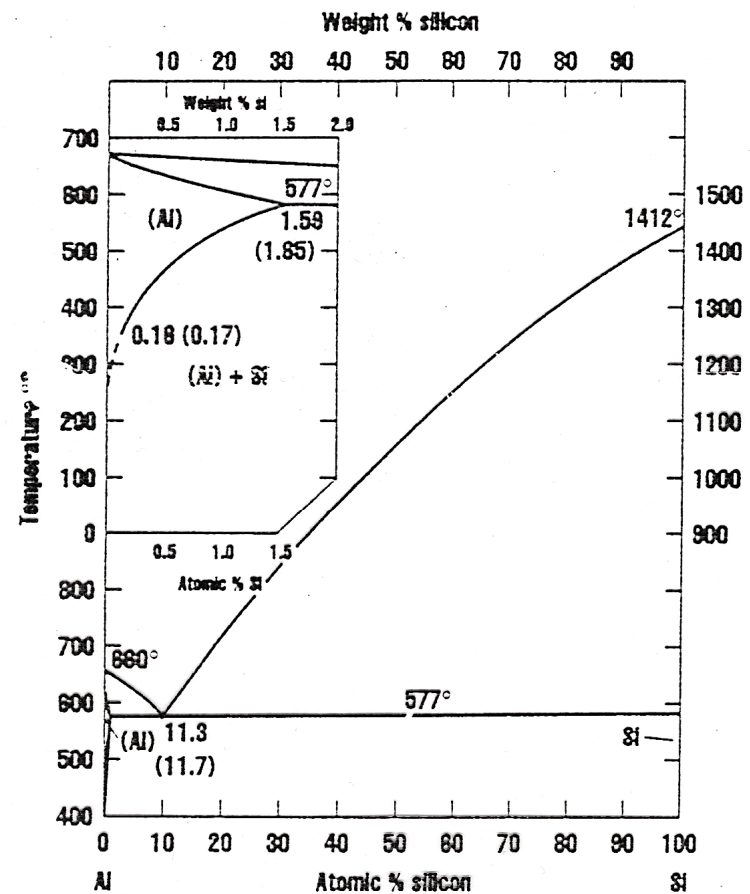


Figure 15-25 Phase diagram of Al/Si. Insert shows the low concentration region.

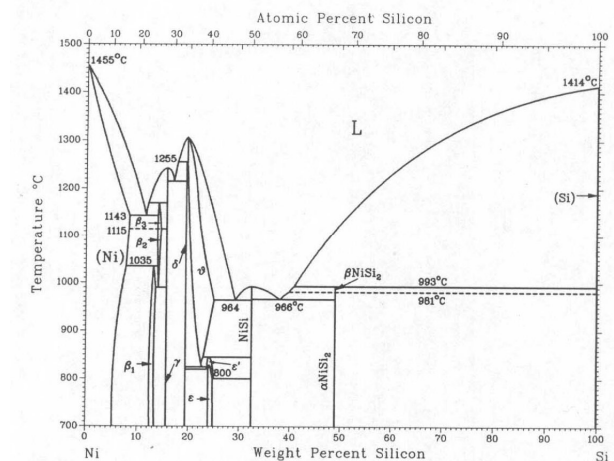
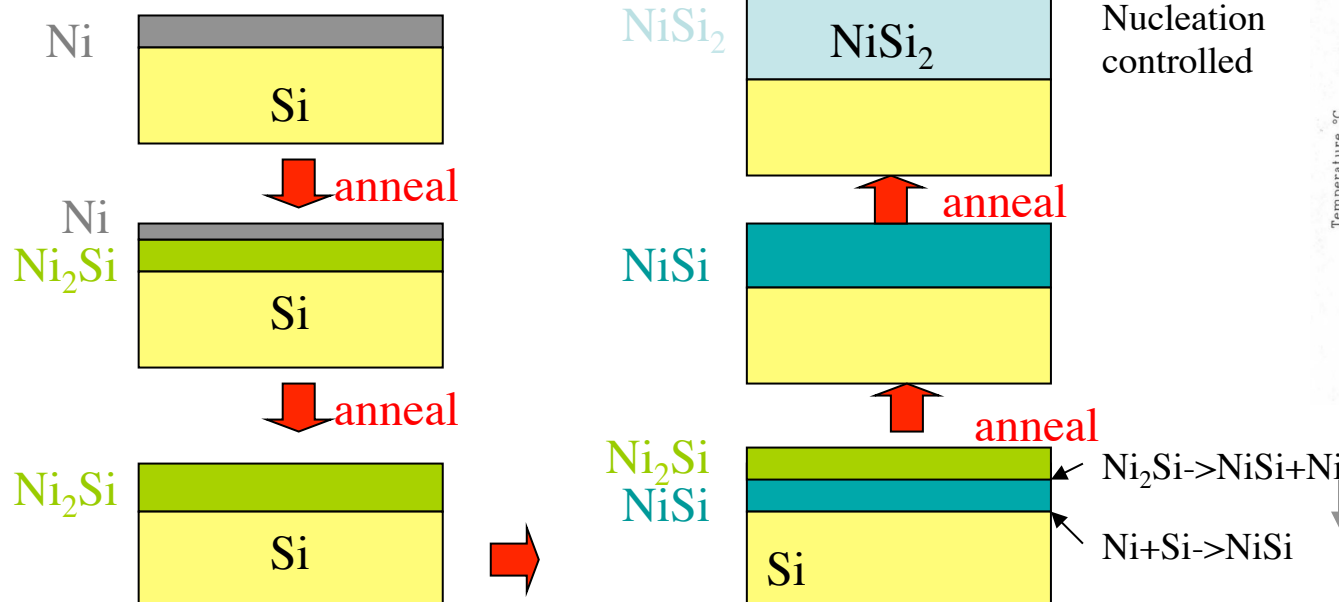
Silicides

Silicides in this context are compounds of one(or more) metallic atom and silicon
 Examples: Ni_2Si , NiSi , NiSi_2 , CoSi_2 , PtSi , IrSi , WSi_2 , Pd_2Si , TiSi_2 ,

Most silicides are metallic, some are reported to be semiconductors (FeSi_2 , $\text{MnSi}_{1.7}$)

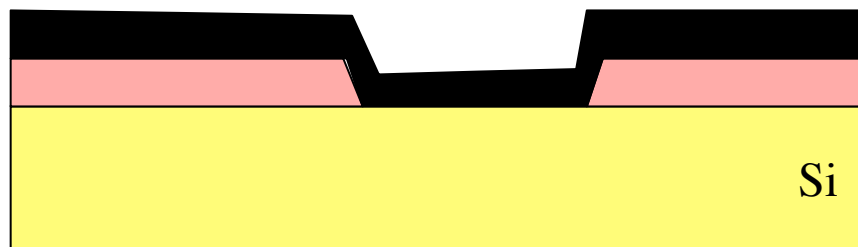
Can be made by reaction of metal film w. Si, Sputtering silicide, (CVD, ALE?)

Example Ni-Si



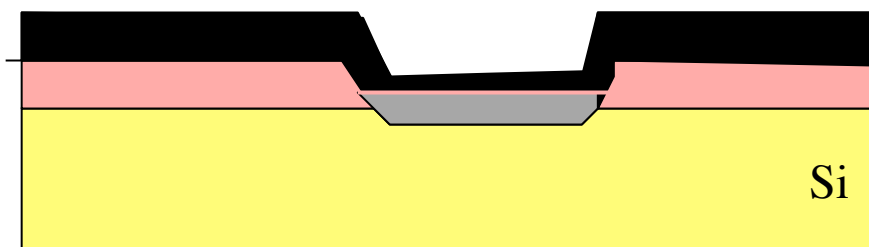
Silicides: example Pt-Si

Used for IR detectors, prev. generation bipolar clamp

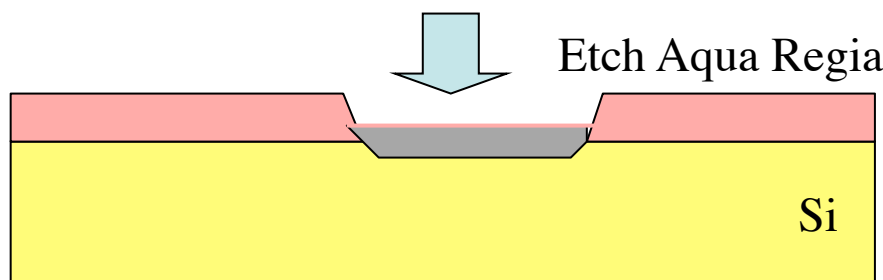


Pt Sputter deposition
SiO₂ (or egun evap w. native oxide)

Anneal 500°C



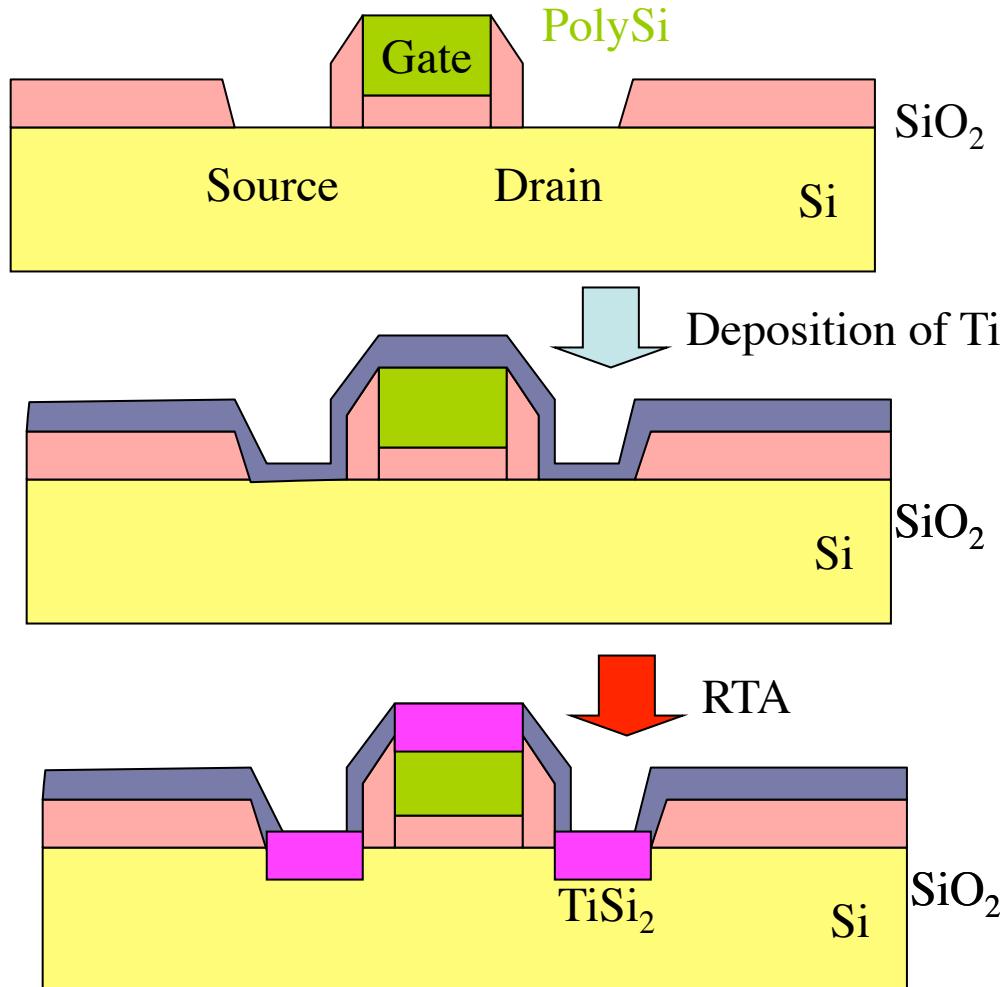
Pt Reaction and diffusion,
SiO₂ Pt₂Si forms first.
 Reaction stops
 by accumulation of SiO₂
 Transforms to PtSi



SiO₂ not etched aqua Regia
Brief dip in HF will remove thin SiO₂

Silicides:Salicide:Ti 1

Used in present generation MOS self-aligned



Si is most mobile specie
Two TiSi₂ phases with different ρ
Nucleation 'difficult' small areas

Silicides:Salicide:Ti 2

Re: diffusing species

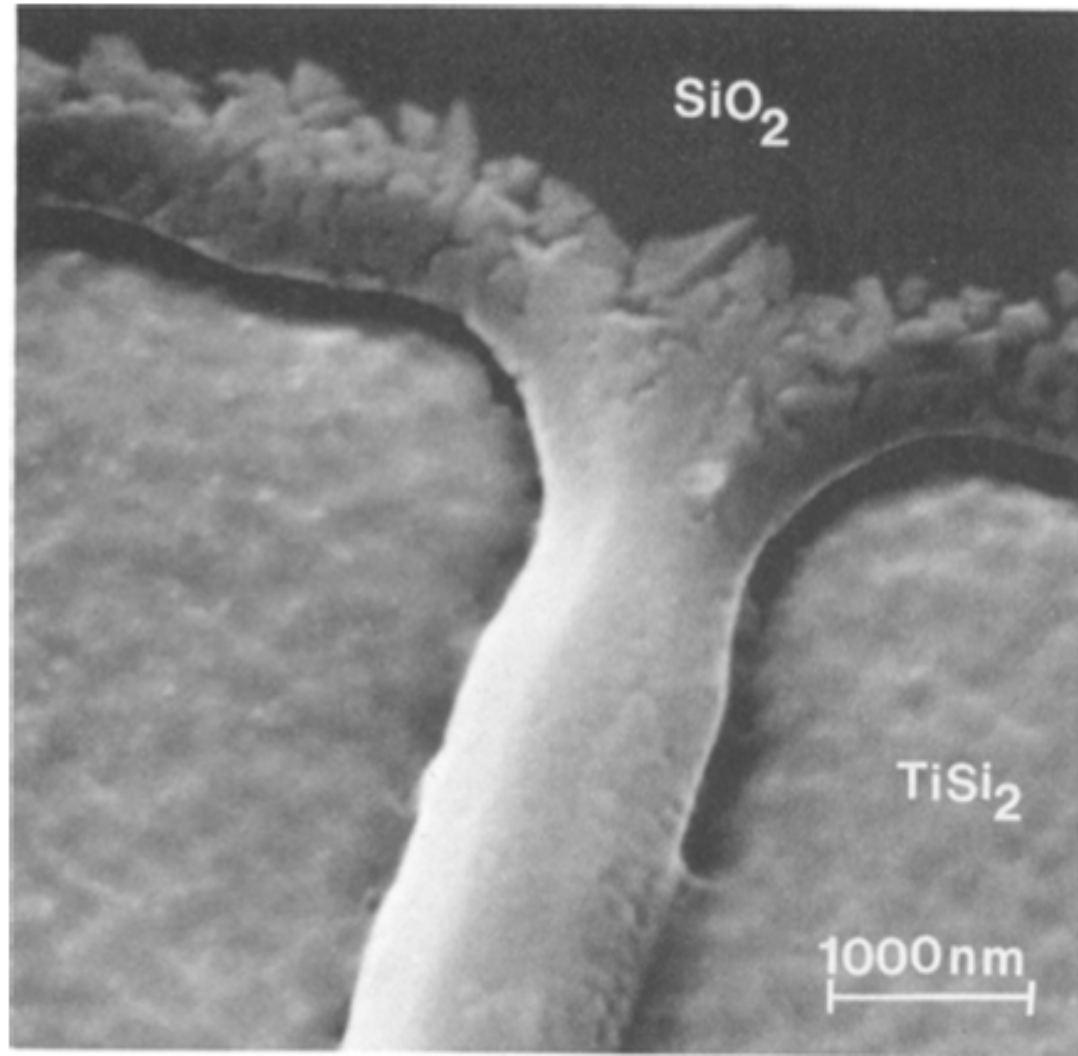


Fig. 8. SEM micrograph of TiSi_2 formed in patterned oxide windows by RTA at 900°C for 10s in argon and followed by a selective Ti etch.

Silicides:NiSi in SiGe MOS

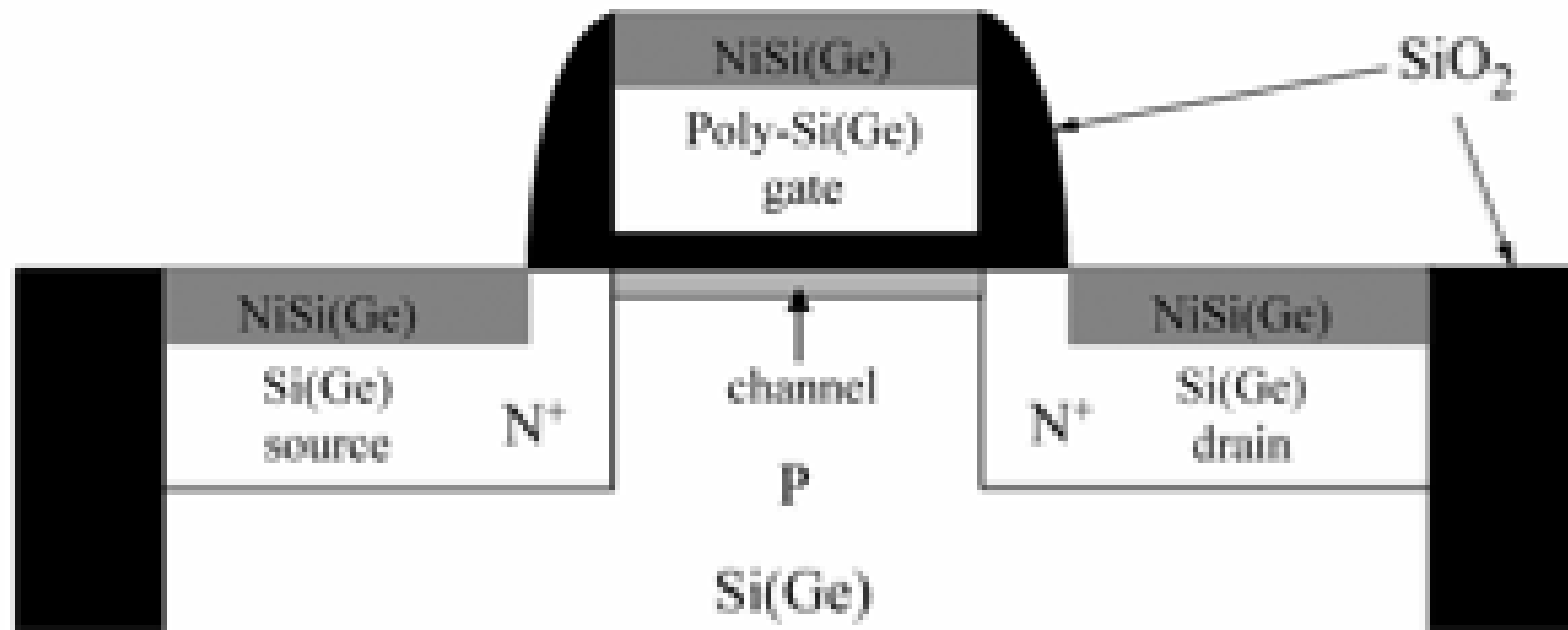


Figure 1. A cross-section of a MOSFET

Silicides:NiSi in SiGe MOS

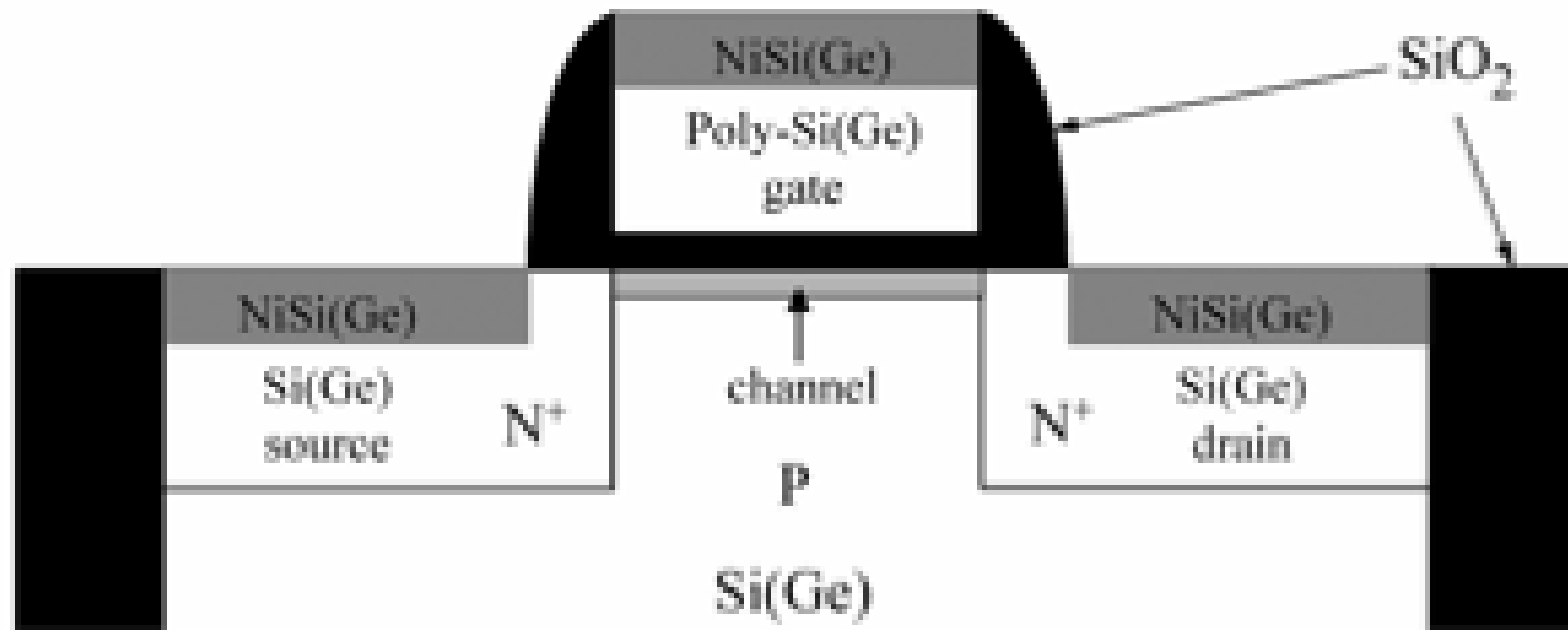
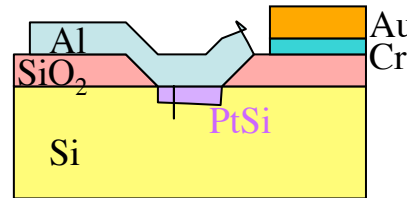


Figure 1. A cross-section of a MOSFET

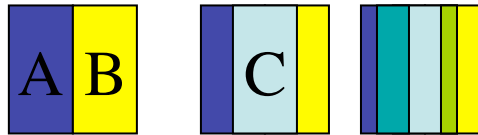
Diffusion barriers

Why do we need them?



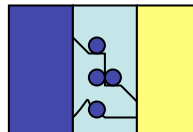
Types

Sacrificial Barriers



$^{AC}_{BC}$

Stuffed Barriers



Amorphous Barriers

Nitride Barriers (TiN)

Electro migration

As phenomenon

Uses outside micro electronics

Significance in microelectronics

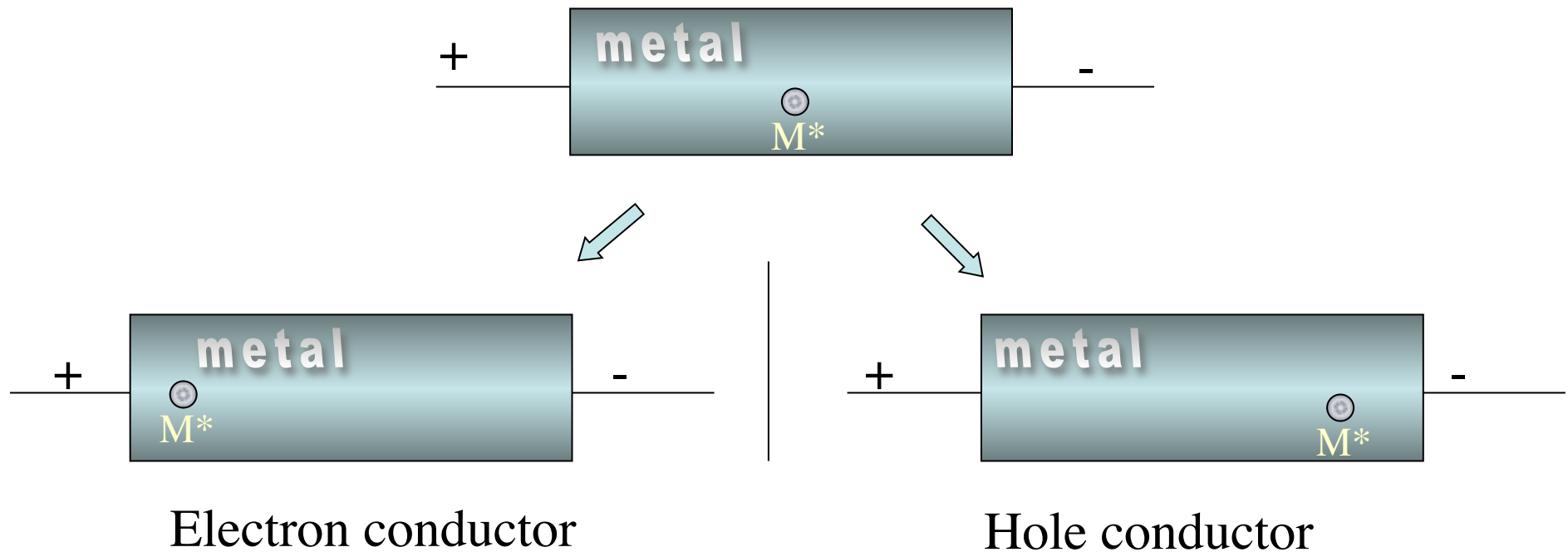
Physical mechanisms

How to measure

Minimizing damaging effects of electro migration

Links [metu](#)

Electro migration as phenomenon

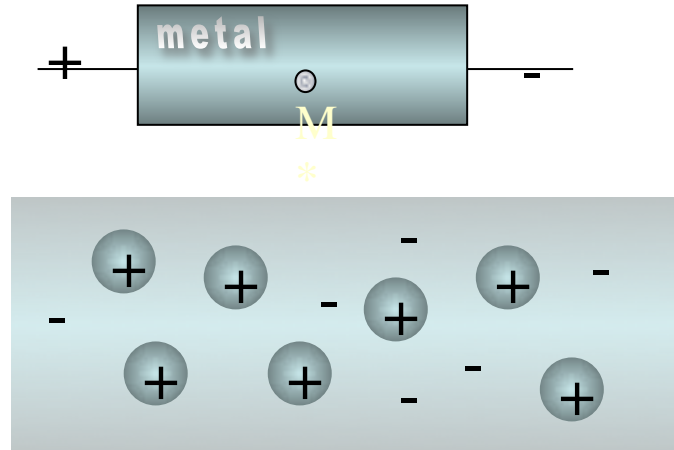


For electrical current $J = qnv = qn\mu\mathcal{E}$ force = $q\mathcal{E}$

For atomic flux, force = $|q|Z^*\mathcal{E}$ Z^* effective charge number

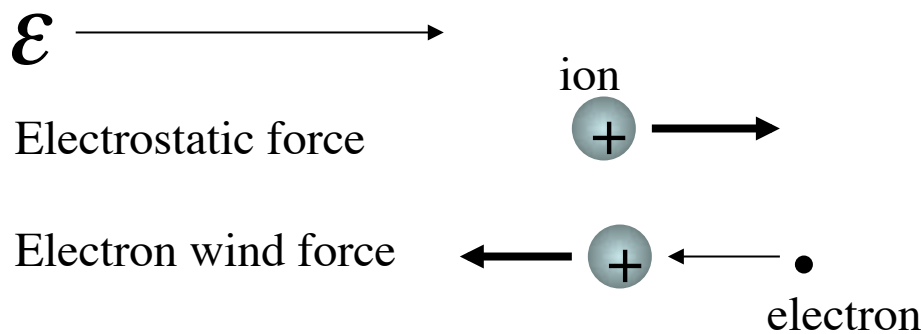
$$Z^* = Z_{\text{elstat}} + Z_{\text{wind}}$$

Electro migration description



$$Z^* = Z_{\text{elstat}} + Z_{\text{wind}}$$

Popularization by jellum model



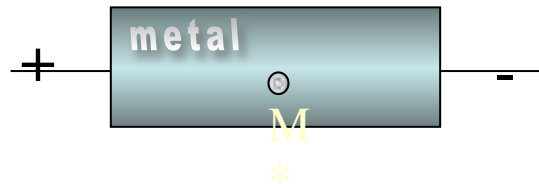
Electron wind force and electrostatic force different direction for electrons

same direction for holes

Can derive electrostatic force flux from the Einstein relation

$$J = N z_1 q D \mathcal{E} / kT \quad (D : \text{diffusivity}, z_1 : \text{effective ion charge number})$$

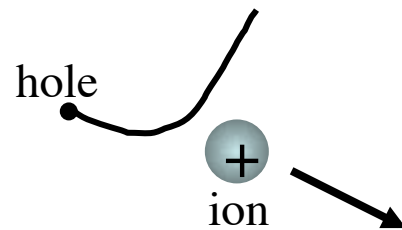
Electron wind force



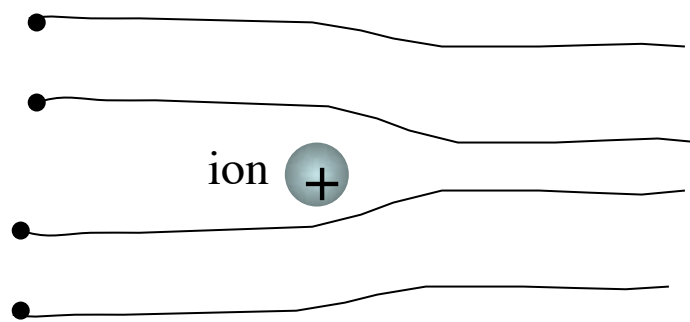
$$Z^* = Z_{\text{elstat}} + Z_{\text{wind}}$$

Ballistic

Electrostatic force



Current divergence induced field



Can derive Z_{wind} in terms of resistivity

Electro migration: uses outside microelectronics

Really none

Could be used for purification of metals

A contributing factor to the initial breakage of light bulbs

Has been used in fundamental studies of Fermi surfaces

Electro migration in thin films

Different than bulk because

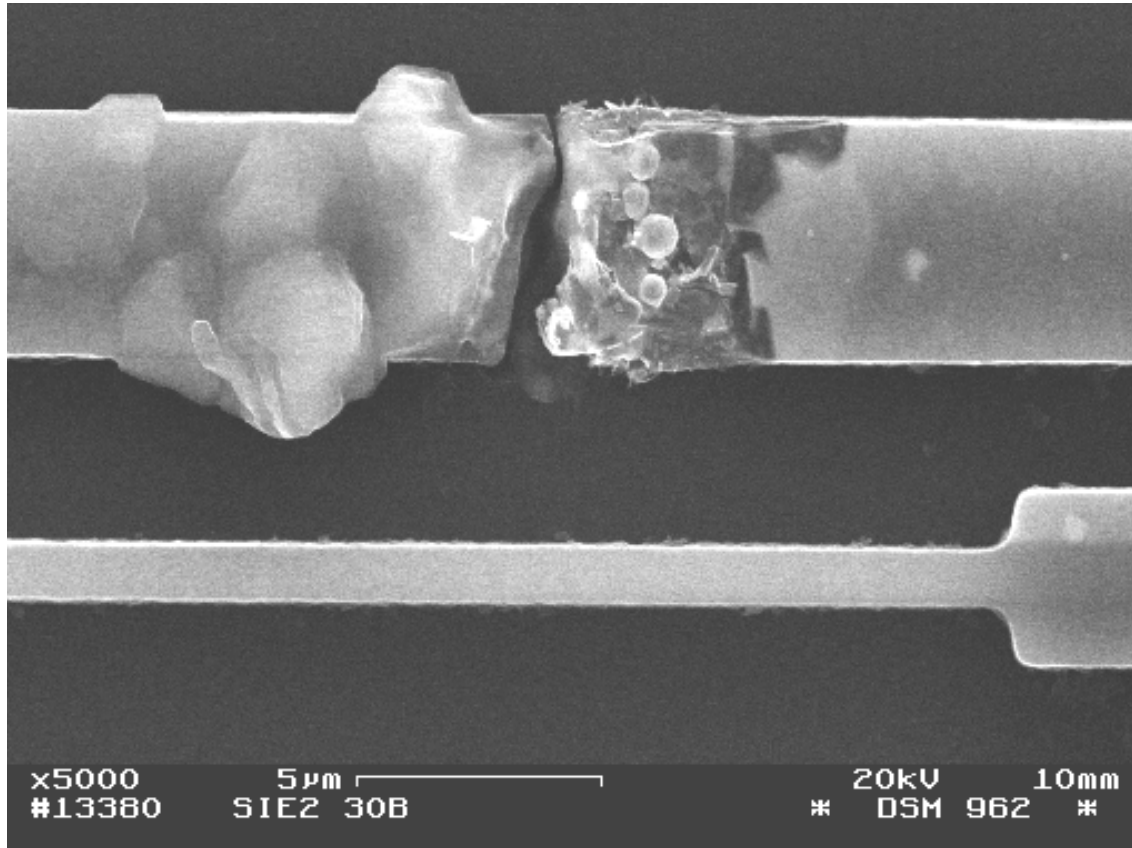
Grain boundaries (and dislocations) diffusion
faster
inhomogeneous

Current inhomogeneities arise easy

Efficient cooling by substrate

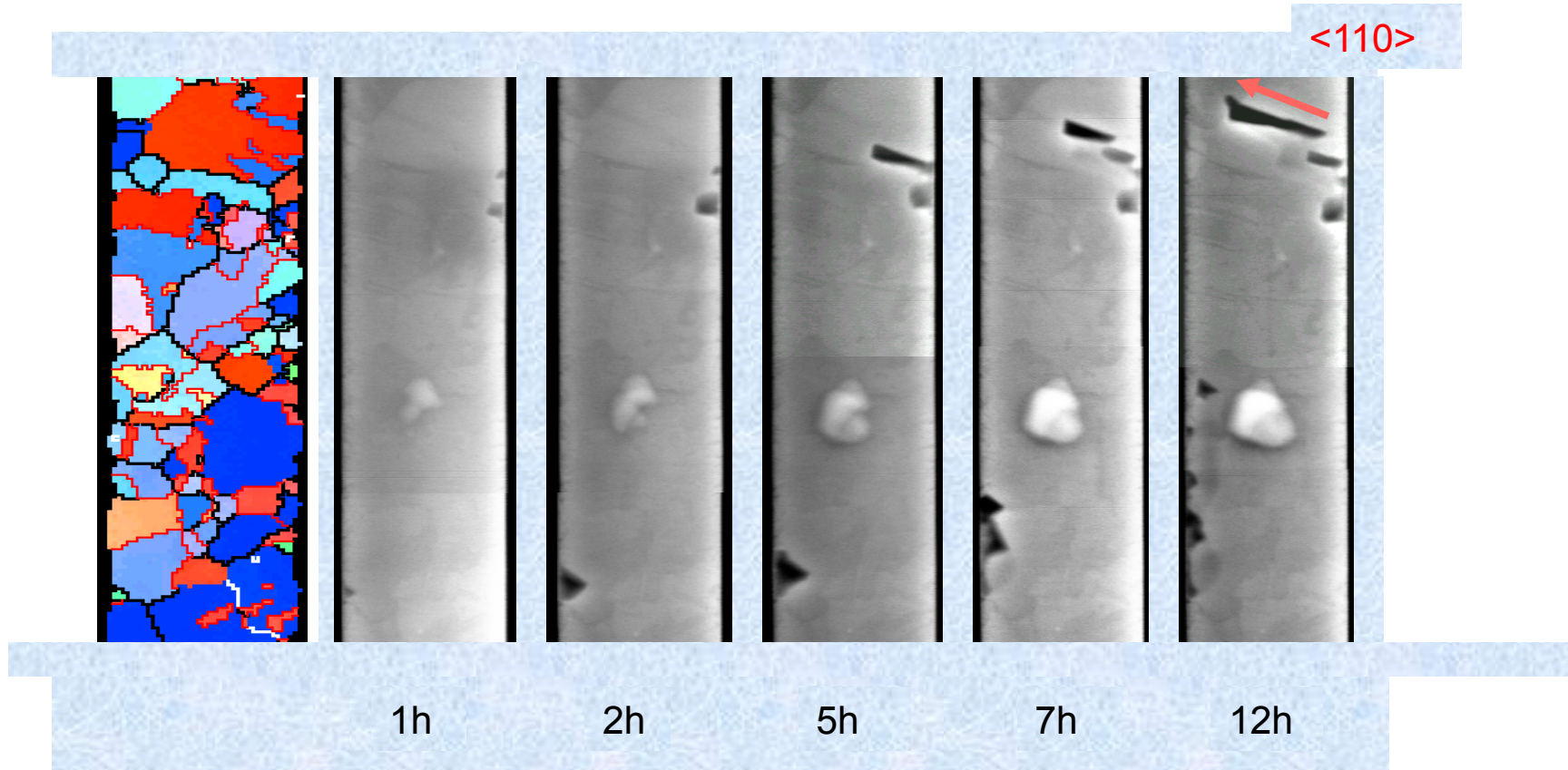
Flux in grain boundary - $1E6 * \text{flux bulk Al in Al at } 175^\circ\text{C}$

Electro migration significance in microelectronics



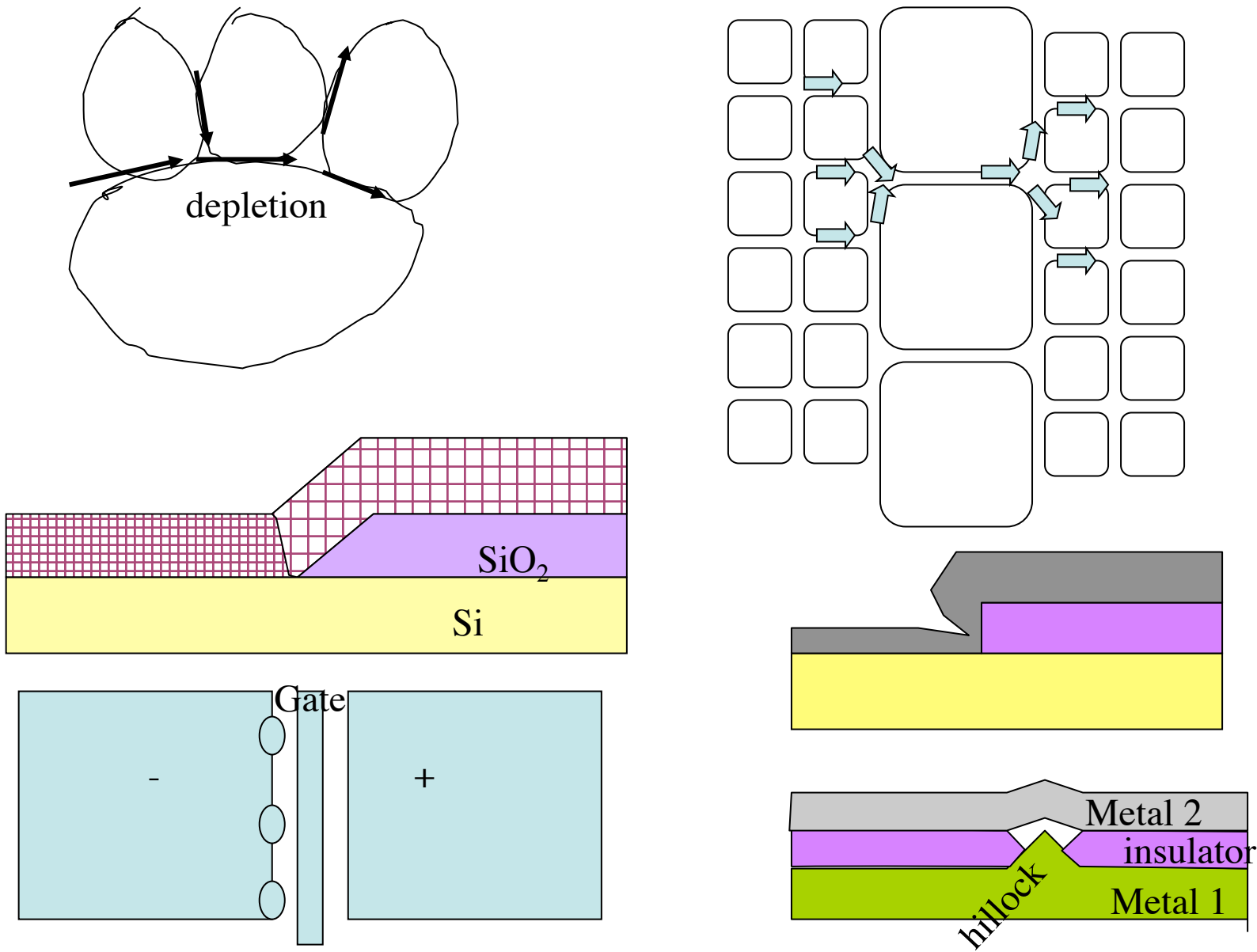
From Michael Zier IFW Dresden(m.zier@ifw-dresden.de),

Electro migration: Significance in microelectronics



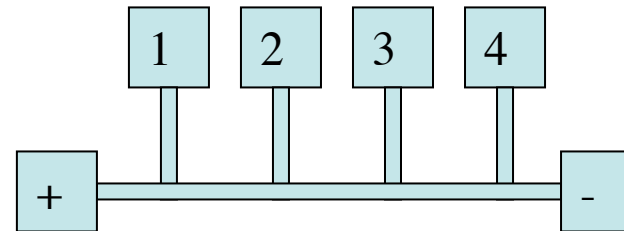
From *IFW Dresden*

Electro migration: Flux divergence



Electro migration: How to measure
Registration of phenomena: SEM
Flux measurement, electron microprobe (EDAX,EDS)

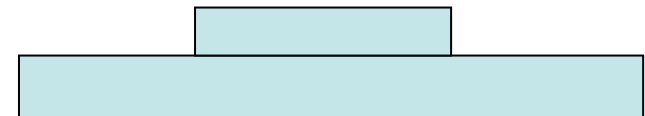
Resistance change



Lifetime measurements, mean time to failure

X-stripe (analogy Kirkendall marker)

By layers



Electro migration: minimizing

Grain engineering

Grain boundary engineering, boundary stuffing

Plug vs caps

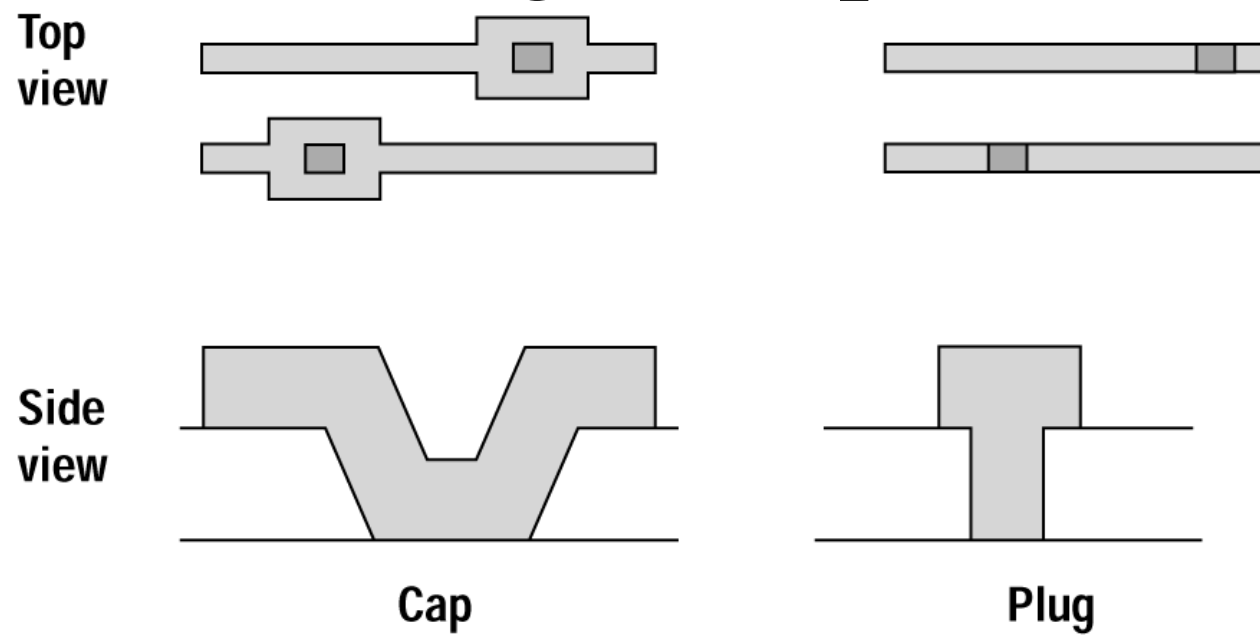


Figure 13.22 The use of caps versus plug-filled contacts.